AD_____
(Leave blank)

Award Number: **W81XWH-07-1-0160**

TITLE: **ATF4, A Novel Mediator of the Anabolic Actions of PTH on Bone**

PRINCIPAL INVESTIGATOR: **Guozhi Xiao, M.D., Ph.D.**

CONTRACTING ORGANIZATION: **University of Pittsburgh**
Pittsburgh, PA 15260

REPORT DATE: **July 2008**

TYPE OF REPORT: **Annual Report**

PREPARED FOR: **U.S. Army Medical Research and Materiel Command**
Fort Detrick, Maryland 21702-5012

DISTRIBUTION STATEMENT: (Check one)

x Approved for public release; distribution unlimited

Distribution limited to U.S. Government agencies only; report contains proprietary information

The views, opinions and/or findings contained in this report are those of the author(s) and should not be construed as an official Department of the Army position, policy or decision unless so designated by other documentation.

REPORT DOCUMENTATION PAGE

Form Approved
OMB No. 0704-0188

Public reporting burden for this collection of information is estimated to average 1 hour per response, including the time for reviewing instructions, searching existing data sources, gathering and maintaining the data needed, and completing and reviewing this collection of information. Send comments regarding this burden estimate or any other aspect of this collection of information, including suggestions for reducing this burden to Department of Defense, Washington Headquarters Services, Directorate for Information Operations and Reports (0704-0188), 1215 Jefferson Davis Highway, Suite 1204, Arlington, VA 22202-4302. Respondents should be aware that notwithstanding any other provision of law, no person shall be subject to any penalty for failing to comply with a collection of information if it does not display a currently valid OMB control number.
PLEASE DO NOT RETURN YOUR FORM TO THE ABOVE ADDRESS.

1. REPORT DATE *(DD-MM-YYYY)*	**2. REPORT TYPE**	**3. DATES COVERED** *(From - To)*
31-07-2008	Annual	1 July 2007 – 30 June 2008

4. TITLE AND SUBTITLE
ATF4, A Novel Mediator of the Anabolic Actions of PTH on Bone

5a. CONTRACT NUMBER
W81XWH-07-1-0160

5b. GRANT NUMBER
PR064047

5c. PROGRAM ELEMENT NUMBER

6. AUTHOR(S)
Guozhi Xiao

Email: xiaog@upmc.edu

5d. PROJECT NUMBER

5e. TASK NUMBER

5f. WORK UNIT NUMBER

7. PERFORMING ORGANIZATION NAME(S) AND ADDRESS(ES)

University of Pittsburgh
Office of Research
350 Thackeray Hall
Pittsburgh, PA 15260

8. PERFORMING ORGANIZATION REPORT NUMBER

9. SPONSORING / MONITORING AGENCY NAME(S) AND ADDRESS(ES)
US Army Medical Research
And Materiel Command
Fort Detrick, MD 21702-5104

10. SPONSOR/MONITOR'S ACRONYM(S)

11. SPONSOR/MONITOR'S REPORT NUMBER(S)

12. DISTRIBUTION / AVAILABILITY STATEMENT

Approved for public release; distribution unlimited

13. SUPPLEMENTARY NOTES

14. ABSTRACT
During the last year of support (from July 1, 2007 to June 30, 2008), our studies have made significant progresses in all aspects of the study: i) we demonstrate that PTH increases ATF4 expression and activity and ATF4 is required for PTH induction of Ocn expression in osteoblasts. ATF4 is a novel downstream target of PTH signaling in osteoblasts; ii) we show that ATF4 is required for the anabolic actions of PTH on bone in vivo, these results were orally presented at the 2007 ASBMR (American Society for Bone and Mineral Research) annual meeting; and iii) We also shows that TFIIAγ increases osteoblast-specific gene expression by facilitating ATF4-Runx2 interactions; Taken together, these data further strongly support our original hypothesis and the specific aims. Two peer-reviewed research papers and two national meeting abstracts are generated from this study during this period of support. In the next year of support, we will: i) determine if ATF4 is required for the anabolic actions of PTH on bone in greater detail; ii) determine if ATF4 is required for PTH regulations of cell proliferation and apoptosis in vitro and in vivo; and iii) determine the role of ATF4-Runx2 interactions in PTH-induced osteoblast function.

15. SUBJECT TERMS
ATF4, Runx2, PTH, anabolism, proliferation, apoptosis

16. SECURITY CLASSIFICATION OF:			**17. LIMITATION OF ABSTRACT**	**18. NUMBER OF PAGES**	**19a. NAME OF RESPONSIBLE PERSON**
a. REPORT	**b. ABSTRACT**	**c. THIS PAGE**			USAMRMC
U	U	U	UU	33	**19b. TELEPHONE NUMBER** *(include area code)*

Table of Contents

Page

This progress report covers research from the period 04/01/07-06/30/08

Introduction

Osteoporosis is a bone disease that affects a large numbers of both men and women including many of our service women and men now in the Armed Forces and VA patients in the United States. It causes a significant amount of morbidity and mortality in patients and is often diagnosed after a fracture occurs. Reducing the risk of osteoporotic and associated fractures of these patients will greatly improve their life quality and survival. Parathyroid hormone (PTH) is the most potent anabolic treatment of osteoporosis currently available. It not only dramatically improves bone mass, but also restores bone microarchitecture and increases bone diameter. All of these mechanisms contribute to increasing bone strength and reducing the risk for fractures. However, the molecular mechanism whereby PTH increases bone formation remains largely unknown. Our central hypotheses in this study are: 1) PTH activates ATF4 by promoting its phosphorylation and protein-protein interactions with Runx2; and 2) ATF4 mediates the anabolic actions of PTH on bone. The long-tern goal of this study has been to elucidate the molecular mechanisms underlying the anabolic actions of PTH on bone. Two Specific Aims have been proposed to determine the functional relationships between ATF4 and PTH actions on bone: 1) determine the mechanism whereby PTH regulates ATF4 transcriptional activity; 2) establish whether the anabolic actions of PTH require ATF4 *in vivo*. Studies determine if ATF4 is required for the anabolic actions of PTH *in vivo* using ATF4-deficient mice. PTH anabolic activity is evaluated in wild type and *Atf4*$^{-/-}$ mice. PTH effects are measured using standard biochemical and histomorphometric criteria.

Body

Task 1: To determine the mechanism by which PTH regulates ATF4 and Runx2 transcriptional activity (1-36 months). In order to determine the role of ATF4 in PTH actions in osteoblasts, we examined effects of PTH on ATF4 expression and activity as well as the requirement for ATF4 in the regulation of *Ocn* by PTH (see P1). PTH elevated levels of ATF4 mRNA and protein in a dose and time-dependent manner (P1-Fig. 1A-C). This PTH regulation requires transcriptional activity, but not *de novo* protein synthesis (P1-Fig. 2A and B). PTH also increased binding of nuclear extracts to OSE1 DNA (P1-Fig. 4A-C). PTH stimulated ATF4-dependent transcriptional activity mainly through PKA with a lesser requirement for PKC and MAPK/ERK pathways (P1-Fig. 5A-C). PTH stimulation of *Ocn* expression was lost by siRNA downregulation of ATF4 in MC-4 cells (P1-Fig. 6A and C) and in *Atf4*$^{-/-}$ bone marrow stromal cells (BMSCs) (P1-Fig. 7C). Collectively, these studies for the first time demonstrate that PTH increases ATF4 expression and activity and that ATF4 is required for PTH induction of *Ocn* expression in osteoblasts. Thus, ATF4 is a novel downstream target of PTH actions in osteoblasts. We defined a novel molecular mechanism mediating ATF4-Runx2 interactions (see P2). We identified general transcription factor IIAγ (TFIIAγ) as a Runx2-interacting factor in a yeast two-hybrid screen. Immunoprecipitation assays confirmed that TFIIAγ interacted with Runx2 in osteoblasts and when coexpressed in COS-7 cell or using purified GST-fusion proteins (P2-Fig. 1A-C). Chromatin immunoprecipitation (ChIP) assay of MC3T3-E1 (clone MC-4) preosteoblast cells showed that in intact cells TFIIAγ was recruited to the region of the *osteocalcin* promoter previously shown to bind Runx2 and ATF4 (P2-Fig. 2). A small region of Runx2 (aa 258-286) was found to be required for TFIIAγ binding (P2-Fig. 1D). While TFIIAγ interacted with Runx2, it did not activate Runx2 (P2-Fig. 3A and B). Instead, TFIIAγ bound to and activates ATF4 (P2-Fig. 3C-H). Further, TFIIAγ together with ATF4

and Runx2 stimulated *osteocalcin* promoter activity (P2-Fig. 5B) and endogenous mRNA expression (P2-Fig. 5A). siRNA silencing of TFIIAγ markedly reduced levels of endogenous ATF4 protein and *Ocn* mRNA in osteoblastic cells (P2-Fig. 6). Overexpression of TFIIAγ increased levels of ATF4 protein (P2-Fig. 7). TFIIAγ significantly prevented ATF4 degradation (P2-Fig. 8). Thus, TFIIAγ functions as a bridging protein linking ATF4 and Runx2. Current study in the project laboratory is determining if PTH regulates the expression of TFIIAγ in osteoblasts.

In addition, expression vectors harboring mutations of potential phosphorylation sites within ATF4 molecule have been successfully generated. The effects of these mutations on ATF4 transcriptional activity and its ability to activate Runx2 as well as on PTH response are being determined in the project laboratory.

A

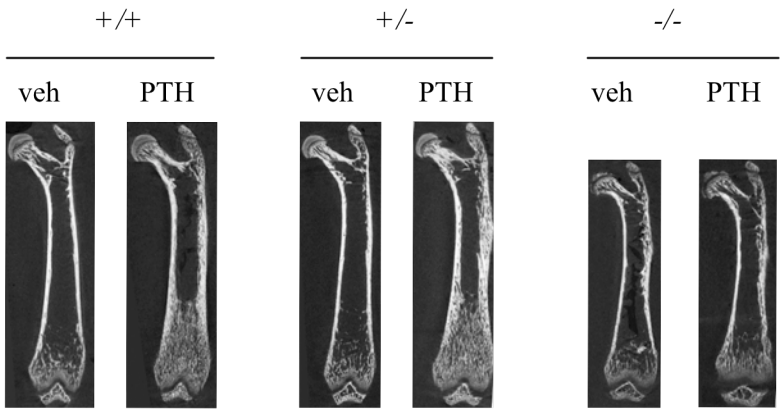

B

	N = 6	N = 6	N = 6	N = 5	N = 6	N = 12
BV/TV(%)	6.2±0.4	33.4±6.6*	6.5±0.5	37.2±4.6*	3.9±0.8	8.6±4.0 *#
TbN(/mm)	1.5±0.08	4.02±0.8*	1.5±0.1	4.7±0.65*	1.3±0.08	2.2±0.6 *#
TbTh(μm)	50.4±5.1	75.5±12*	54.1±2.6	76.8±4.4*	48.3±6.9	54.4±4.2 *#
TbSp(mm)	0.67±0.04	0.27±0.1*	0.66±0.05	0.25±0.04*	0.78±0.06	0.50±0.13 *#
Cort.Th(mm)	0.19±0.06	0.37±0.01*	0.17±0.01	0.40±0.08*	0.13±0.01	0.17±0.02 *#

Fig. 1. ATF4 deficiency severely impairs the anabolic effects of PTH on femurs. A, two-dimensional reconstruction from μCT scan of distal femurs from 5-day-old *wt*, *Atf4*$^{+/-}$ and *Atf4*$^{-/-}$ mice with and without intermittent PTH for 28 d are shown. **B**, quantitative analysis of effects of PTH on bone volume/tissue volume (BV/TV), trabecular number (Tb. N), trabecular thickness (Tb.Th), trabecular space (Tb.Sp), and cortical thickness (Cort. Th). *P<0.05 (veh vs. PTH), #P<0.05 (PTH/veh-wt vs. PTH/veh-*Atf4*$^{-/-}$).

<u>*Task 2: To establish whether the anabolic actions of PTH require ATF4 (6-48 months).*</u> In vivo, we examined if ATF4 is required for the anabolic actions of PTH on bone using an *Atf4*$^{-/-}$ mouse model. Five-day-old w*t*, *Atf4*$^{+/-}$, and *Atf4*$^{-/-}$ mice were given daily subcutaneous injections of vehicle (saline) or hPTH(1-34) (60 ng/g body weight) for 28 days. In *wt* mice, μCT analyses of femurs show PTH significantly increased BV/TV, Tb.N, and Tb.Th in *wt* femurs by 4.4-fold, 1.7-fold, and 50%,

respectively, and decreased Tb.Sp by 1.5-fold (P<0.05, veh vs. PTH). In contrast, PTH only elevated BV/TV, Tb.N, and Tb.Th in *Atf4*$^{-/-}$ mice by 1.2-fold, 69%, and 12.6%, respectively, and decreased Tb.Sp by 56%. The PTH fold stimulations for all trabecular parameters were significantly decreased in *Atf4*$^{-/-}$ mice relative to *wt* mice (P<0.05, PTH/veh-*wt* vs. PTH/veh-*Atf4*$^{-/-}$)(Fig. 1). PTH increased Cort.Th in *wt* femurs by 70% (P<0.05, veh vs. PTH), which was significantly reduced to 21% in *Atf4*$^{-/-}$ mice (P<0.05, PTH/veh-*wt* vs. PTH/veh-*Atf4*$^{-/-}$)(Fig. 1). PTH similarly affected all trabecular and cortical parameters in *Atf4*$^{+/+}$ and *Atf4*$^{+/-}$ mice (Fig. 1). For this reason, subsequent experiments only compared the PTH effects between *wt* and *Atf4*$^{-/-}$ mice. Histological analyses show that PTH displayed potent anabolic effects on tibiae, vertebrae, and calvariae, which were significantly reduced in *Atf4*$^{-/-}$ mice) (Fig. 2). At the molecular level, PTH markedly increased levels of osteocalcin (*Ocn*) and bone sialoprotein (*Bsp*) mRNA of long bones as measured by quantitative real-time RT/PCR). This increase was significantly reduced in the absence of ATF4 (Fig. 3B and C). In contrast, level of c-Fos was not altered PTH or ATF4 deficiency. Thus, ATF4 is required for the PTH anabolic actions in bone.

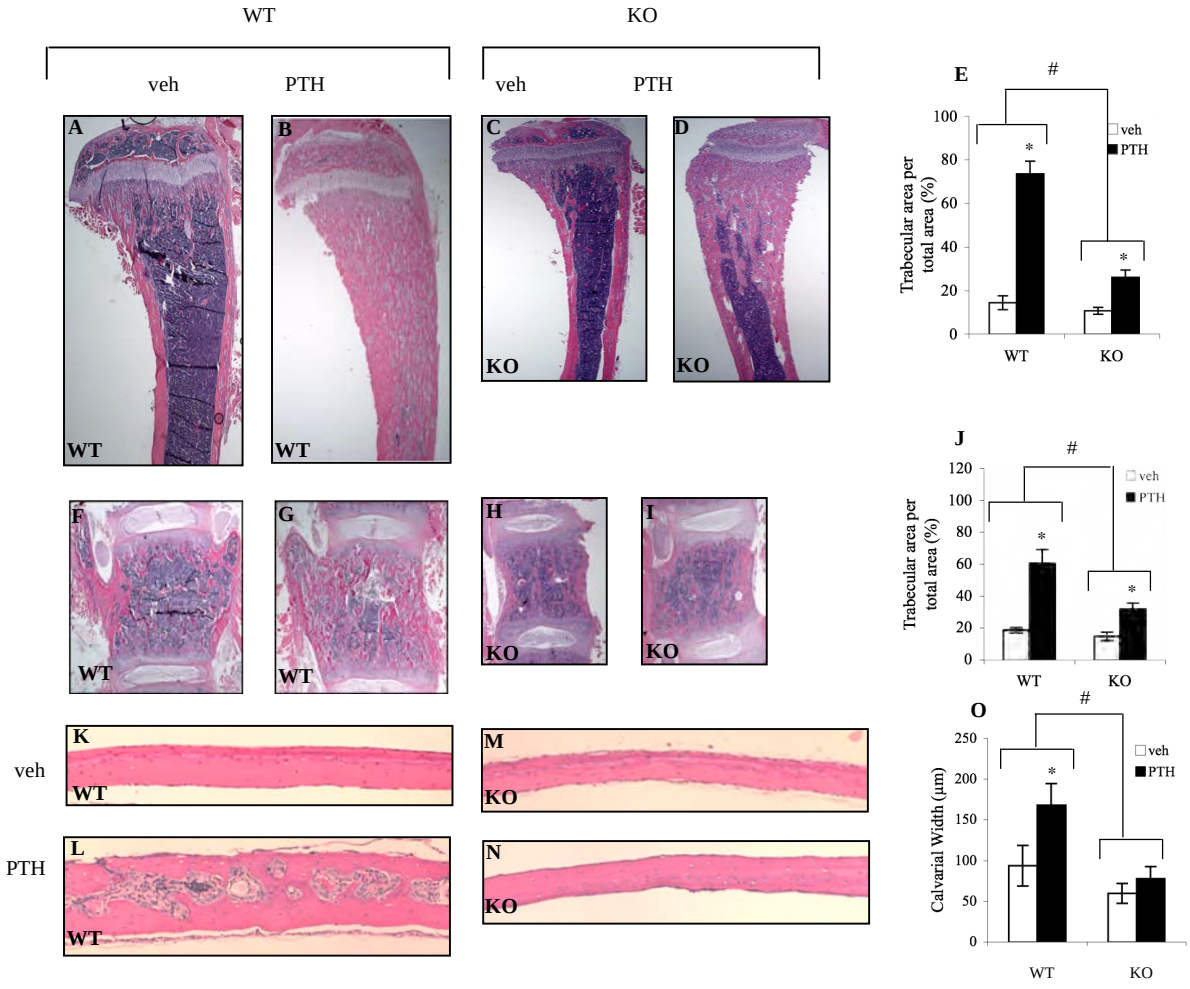

Fig. 2. PTH-stimulated bone formation in tibiae, vertebrae, and calvariae is significantly diminished in *Atf4*$^{-/-}$ mice. Mice were treated as in Fig. 1. A-E, tibiae; F-J, lumber vertebrae; K-O, calvariae. Representative H&E stained section are shown. Data represent mean±S.D. *P<0.05 (veh vs. PTH), $^{\#}$P<0.05 (PTH/veh-wt vs. PTH/veh-*Atf4*$^{-/-}$).

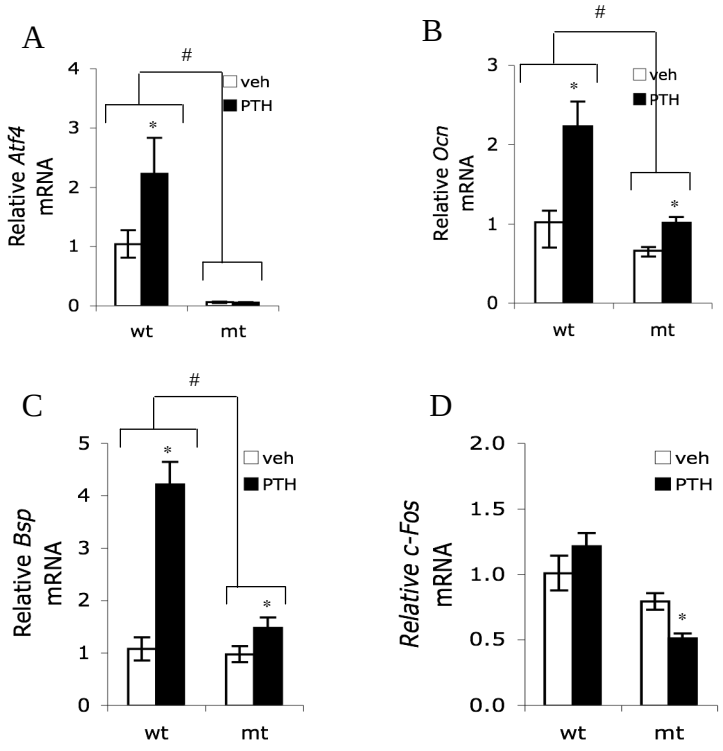

Fig. 3. ATF4 deficiency reduces PTH-induced osteoblast differentiation in vivo. Mice were treated as in Fig. 1. Total RNAs were isolated from tibiae and analyzed by quantitative real-time RT-PCR using specific primers for *Atf4*, *Ocn*, *Bsp*, and *c-Fos mRNAs, which* were normalized to *Gapdh* mRNA. Data are presented as mean ± SD. *P<0.05 (veh vs. PTH), $^{\#}$P<0.05 (PTH/veh-wt vs. PTH/veh-*Atf4*$^{-/-}$).

Key Research Accomplishments

- ATF4 expression vectors that contain mutations of potential phosphorylation sites within ATF4 molecule have been constructed. The effects of these mutations on ATF4 transcriptional activity and its ability to activate Runx2 as well as the PTH response are being determined in the project laboratory.
- PTH increases ATF4 expression and activity and ATF4 is required for PTH induction of *Ocn* expression in osteoblasts. Therefore, ATF4 is a novel downstream target of PTH signaling in osteoblasts (see P1).
- TFIIAγ increases osteoblast-specific gene expression by facilitating ATF4-Runx2 interactions (see P2).
- We have successfully established several in vivo assays for osteoblast activity and bone formation, including H&E staining, in vivo osteoblast proliferation assay (BrdU staining of bone tissue sections), in vivo bone formation assay (calcein labeling), and in vivo apoptosis assay of bone tissues. Using these assays, our preliminary study shows that ATF4 is required for the anabolic actions of PTH on bone in vivo (see A1).

Reportable Outcomes

Peer-reviewed papers:

P1. Yu S, Franceschi RT, Luo M, Zhang X, Jiang D, Lai Y, Jiang Y, Zhang J, Xiao G (2008). Parathyroid hormone increases activating transcription factor 4 expression and activity in osteoblasts: requirement for *osteocalcin* gene expression. Endocrinology, 2008; 149(4): 1960-8.

P2. Yu S, Jiang Y, Galson DL, Luo M, Lai Y, Lu Y, Ouyang HJ, Zhang J, Xiao G (2008). General transcription factor IIA-gamma increases osteoblast-specific osteocalcin gene expression via activating transcription factor 4 and runt-related transcription factor 2. J Biol Chem. 2008; 283(9): 5542-53.

Abstracts:

A1. Yu S, Luo M, Franceschi RT, Jiang D, Zhang J, Patrene K, Hankenson KD, Roodman GD, Xiao G. ATF4 Is Required for the Anabolic Actions of PTH on Bone in vivo. J. Bone Min. Res., 22:1007 (2007 ASBMR Oral Presentation).

A2. Yu S, Jiang Y, Luo M, Lu Y, Zhang J, Roodman GD, G. Xiao G. TFIIA, ATF4, and Runx2 Synergistically Activate Osteoblast-specific Osteocalcin Gene Expression (2007-ASBMR poster)

Conclusion

During the last year of support, our studies establish that: i) PTH increases ATF4 expression and activity and ATF4 is required for PTH induction of *Ocn* expression in osteoblasts. ATF4 is a novel downstream target of PTH signaling in osteoblasts; ii) ATF4 is required for the anabolic actions of PTH on bone in vivo; iii) TFIIAγ increases osteoblast-specific gene expression by facilitating ATF4-Runx2 interactions; and iv) ATF4 mutation constructs have been generated and several in vivo bone formation assays have been successfully developed.

The knowledge obtained from these studies will significantly enhance our understanding of the molecular mechanism underlying the actions of PTH in osteoblasts and bone and define new potential therapeutic targets for improved treatment of osteoporosis and other metabolic bone diseases.

References

N/A

Appendices

Two peer-reviewed research papers: P1, P2
Three national meeting abstracts: A1, A2

0013-7227/08/$15.00/0
Printed in U.S.A.

Endocrinology 93(4):0000–0000
Copyright © 2008 by The Endocrine Society
doi: 10.1210/en.2007-1573

Parathyroid Hormone Increases Activating Transcription Factor 4 Expression and Activity in Osteoblasts: Requirement for *Osteocalcin* Gene Expression

Shibing Yu, Renny T. Franceschi, Min Luo, Xiaoyan Zhang, Di Jiang, Yumei Lai, Yu Jiang, Jian Zhang, and Guozhi Xiao

Departments of Medicine (S.Y., M.L., X.Z., Y.L., J.Z., G.X.) and Pharmacology (Y.J.), University of Pittsburgh, Pittsburgh, Pennsylvania 15240; and Departments of Periodontics and Oral Medicine (R.T.F., D.J.), School of Dentistry, and Department of Biological Chemistry (R.T.F.), School of Medicine, University of Michigan, Ann Arbor, Michigan 48109

PTH is an important peptide hormone regulator of calcium homeostasis and osteoblast function. However, its mechanism of action in osteoblasts is poorly understood. Our previous study demonstrated that PTH activates mouse *osteocalcin (Ocn)* gene 2 promoter through the osteoblast-specific element 1 site, a recently identified activating transcription factor-4 (ATF4) -binding element. In the present study, we examined effects of PTH on ATF4 expression and activity as well as the requirement for ATF4 in the regulation of *Ocn* by PTH. Results show that PTH elevated levels of ATF4 mRNA and protein in a dose- and time-dependent manner. This PTH regulation requires transcriptional activity but not *de novo* protein synthesis. PTH also increased binding of nuclear extracts to osteoblast-specific element 1 DNA. PTH stimulated ATF4-dependent transcriptional activity mainly through protein kinase A with a lesser requirement for protein kinase C and MAPK/ERK pathways. Lastly, PTH stimulation of *Ocn* expression was lost by silent interfering RNA down-regulation of ATF4 in MC-4 cells and *Atf4*$^{-/-}$ bone marrow stromal cells. Collectively, these studies for the first time demonstrate that PTH increases ATF4 expression and activity and that ATF4 is required for PTH induction of *Ocn* expression in osteoblasts. (*Endocrinology* 93: 0000–0000, 2008)

AQ: A

PTH IS A MAJOR regulator of osteoblast activity and skeletal homeostasis. PTH has both catabolic and anabolic effects on osteoblasts and bone that depend on the temporal pattern of administration; continuous administration decreases bone mass, whereas intermittent administration increases bone mass (1–3). At the molecular level, PTH binds to the PTH-1 receptor (PTH1R), a G protein-coupled receptor that is expressed in osteoblasts (4–6) and activates multiple intracellular signaling pathways that involve cAMP, inositol phosphates, intracellular Ca^{2+}, protein kinases A and C (7), and the ERK/MAPK pathway (8, 9). The ability of PTH to regulate gene expression is largely dependent on activation of specific transcription factors such as cAMP response element binding protein (CREB) (10, 11), activator protein-1 family members (12–15), pituitary-specific transcription factor-1 (16), and Runt-related transcription factor-2 (Runx2) (12, 17). A better understanding of the downstream PTH signaling events is essential to understand the mechanistic basis for the anabolic and catabolic actions of this hormone on bone.

AQ: B

The *osteocalcin* (*Ocn*) promoter has been the major paradigm for unraveling the mechanisms mediating osteoblast-specific gene expression and defining a number of transcription factors and cofactors (18–29). Because *Ocn* gene is regulated by PTH (30–32), we considered it a good model for identifying new transcriptional mediators of PTH action. Using this system, we recently showed that the osteoblast-specific element (OSE)-1 in the proximal mouse *(Ocn)* gene 2 (mOG2) promoter (19) is necessary and sufficient for PTH induction of this gene (33). Immediately after publication of this study, the OSE1 was identified as a binding site for activating transcription factor-4 (ATF4) (34).

ATF4, also known as CREB2 (35) and tax-responsive enhancer element B67 (36), is a member of the ATF/CREB family of leucine-zipper factors that also includes CREB, cAMP response element modulator, ATF1, ATF2, ATF3, and ATF4 (37–41). These proteins bind to DNA via their basic region and dimerize via their leucine domain to form a large variety of homodimers and/or heterodimers that allow the cell to coordinate signals from multiple pathways (37–41). An *in vivo* role for ATF4 in bone development was established using *Atf4*-deficient mice (29). ATF4 is required for expression of *Ocn* and *bone sialoprotein* as demonstrated by the dramatic reduction of their mRNAs in *Atf4*$^{-/-}$ bone (29). ATF4 activates *Ocn* transcription through direct binding to the OSE1 site as well as interactions with Runx2 through

First Published Online January 10, 2008

Abbreviations: ActD, Actinomycin D; ATF4, activating transcription factor 4; BMSC, bone marrow stromal cell; CHX, cycloheximide; CRE, cAMP response element; CREB, CRE binding protein; FBS, fetal bovine serum; FSK, forskolin; GMSA, gel mobility shift assay; MC-4, MC3T3-E1 subclone 4; mOG2, mouse *Ocn* gene 2; mt, mutant; OCN, osteocalcin; OSE1, osteoblast-specific element-1; PKA, protein kinase A; PKC, protein kinase C; PMA, phorbol 12-myristate 13-acetate; PTH1R, PTH-1 receptor; RSK2, ribosomal kinase 2; Runx2, Runt-related transcription factor-2; siRNA, small interfering RNA; wt, wild type.

***Endocrinology* is published monthly by The Endocrine Society (http://www.endo-society.org), the foremost professional society serving the endocrine community.**

balt3/zee-end/zee-end/zee00408/zee3966-08a | eideg | S=4 | 2/1/08 | 14:49 | Art: EN-07-1573 | Input-ss

cooperative interactions with OSE1 and OSE2 (also known as nuclear matrix protein 2 binding site) sites in the promoter (19, 20, 25). ATF4 activity is negatively regulated by factor inhibiting activating transcription factor-4-mediated transcription (42). factor inhibiting activating transcription factor binds to ATF4 and represses its activity and bone formation *in vivo*. Although *Atf4* mRNA is ubiquitously expressed, ATF4 protein preferentially accumulates in osteoblasts (34). This accumulation is explained by a selective reduction of proteasomal degradation in osteoblasts.

The purpose of this study was to determine the effects of PTH on ATF4 expression and activity and evaluate whether ATF4 mediates PTH induction of *Ocn* expression in osteoblasts.

Materials and Methods

Reagents

Tissue culture media and fetal bovine serum were obtained from HyClone (Logan, UT). γ-[^{32}P]ATP (3000 Ci/mmol) and α-[^{32}P]dCTP (3000 Ci/mmol) were purchased from GE Healthcare (Piscataway, NJ). Other reagents were obtained from the following sources: H89, forskolin (FSK), GF109203X, phorbol 12-myristate 13-acetate (PMA), cycloheximide (CHX), actinomycin D (ActD), and mouse monoclonal antibody against β-actin from Sigma (St. Louis, MO); U0126 from Promega (Madison, WI); and U0124 from Calbiochem (La Jolla, CA), PTH (1–34) from Bachem (Torrance, CA), antibodies against ATF4, Runx2, and horseradish peroxidase-conjugated mouse or goat IgG from Santa Cruz (Santa Cruz, CA). All other chemicals were of analytical grade.

Cell cultures

Mouse MC3T3-E1 subclone 4 (MC-4) cells were described previously (43, 44) and maintained in ascorbic acid-free α-MEM, 10% fetal bovine serum (FBS), and 1% penicillin/streptomycin and were not used beyond passage 15. Rat osteoblast-like UMR106–01 cells (45) were maintained in DMEM and 10% FBS. Isolation of mouse primary bone marrow stromal cells (BMSCs) was described previously (33). Briefly, 6-wk-old male C57BL/6 mice were killed by cervical dislocation. Tibiae and femurs were isolated and the epiphyses were cut. Marrow was flushed with DMEM containing 20% FBS, 1% penicillin/streptomycin, and 10^{-8} M dexamethasone into a 60-mm dish, and the cell suspension was aspirated up and down with a 20-gauge needle to break clumps of marrow. The cell suspension (marrow from two mice/flask) was then cultured in a T75 flask in the same medium. After 10 d, cells reach confluency and are ready for experiments.

DNA constructs and transfection

Wild-type and mutant p4OSE1-luc plasmids were described previously (25, 33). Cells were plated on 35-mm dishes at a density of 5×10^4 cells/cm^2. After 24 h, cells were transfected with lipofectAMINE 2000 (Invitrogen, Carlsbad, CA) according to the manufacturer's instructions. Each transfection contained 0.5 μg of the indicated plasmid plus 0.05 μg of pRL-SV40, containing a cDNA for Renilla reformis luciferase to control for transfection efficiency. Cells were harvested and assayed using the dual luciferase assay kit (Promega) on a Monolight 2010 luminometer (BD Biosciences, San Diego, CA).

AQ: C

Preparation of nuclear extracts and gel mobility shift assay (GMSA)

Nuclear extracts were prepared and GMSAs were conducted as previously described (43). Each reaction contained 1 μg of nuclear extracts. The DNA sequences of OSE1 oligonucleotides used for GMSA were as follows: wild-type (wt): TGC TTA CAT CAG AGA GCA); mutant (mt): TGC TTA gta CAG AGA GCA.

Western blot analysis

Twenty micrograms of nuclear extracts were fractionated on a 10% SDS-PAGE gel and transferred onto nitrocellulose membranes (Schleicher & Schuell, Keene, NH). The membrane was blocked in 5% nonfat milk in Tris-buffered saline/Tween 20 buffer; probed with antibodies against ATF4 (1:1000) followed by incubation with secondary antibodies conjugated with horseradish peroxidase (1:5000); and visualized using an enhanced chemiluminescence kit (Pierce, Rockford, IL). Finally, blots were stripped two times in buffer containing 65 mM Tris Cl (pH 6.8), 2% sodium dodecyl sulfate, and 0.7% (vol/vol) β-mercaptoethanol at 65 C for 15 min and reprobed with β-actin antibody (1:5000) for normalization.

RNA isolation and reverse transcription

Total RNA was isolated using TRIzol reagent (Invitrogen Life Technologies, Gaithersburg, MD) according to the manufacturer's protocol. Reverse transcription was performed using 2 μg of denatured RNA and 100 pmol of random hexamers (Applied Biosystems, Foster, CA) in a total volume of 25 μl containing 12.5 U MultiScribe reverse transcriptase (Applied Biosystems) according to the manufacturer's instructions.

Quantitative real-time PCR

Quantitative real-time PCR was performed on an iCycler (Bio-Rad, Minneapolis, MN) using a SYBR Green PCR core kit (Applied Biosystems) and cDNA equivalent to 10 ng RNA in a 50-μl reaction according to the manufacturer's instructions. The DNA sequences of mouse primers used for real-time PCR were: *Atf4*, 5′-GAG CTT CCT GAA CAG CGA AGT G-3′ (forward), 5′-TGG CCA CCT CCA GAT AGT CAT C-3′ (reverse); *Ocn*, 5′-TAG TGA ACA GAC TCC GGC GCT A-3′ (forward), 5′-TGT AGG CGG TCT TCA AGC CAT-3′ (reverse); *Pth1r*, 5′-GAT GCG GAC GAT GTC TTT ACC-3′ (forward), 5′-GGC GGT CAA ATA CCT CC-3′ (reverse); *Col1(I)*, 5′-AGA TTG AGA ACA TCC GCA GCC-3′ (forward), 5′-TCC AGT ACT CTC CGC TCT TCC A-3′ (reverse); *Opn*, 5′-CCA ATG AAA GCC ATG ACC ACA-3′, (forward), 5′-CGT CAG ATT CAT CCG AGT CCA C-3′ (reverse); *Gapdh*, 5′-CAG TGC CAG CCT CGT CCC GTA GA-3′ (forward), 5′-CTG CAA ATG GCA GCC CTG GTG AC-3′ (reverse). For all primers the amplification was performed as follows: initial denaturation at 95 C for 10 min followed by 40 cycles of 95 C for 15 sec and 60 C for 60 sec. Melting curve analysis was used to confirm the specificity of the PCR products. Six samples were run for each primer set. The levels of mRNA were calculated by the ΔCT method (46). *Atf4*, *Ocn*, *Col1(I)*, *Pth1r*, and *Opn* mRNAs were normalized to *Gapdh* mRNA.

AQ: D

Northern blot

Twenty micrograms of total RNA was fractionated on 1.0% agarose-formaldehyde gels and blotted onto nitrocellulose paper. The mouse *Atf4* cDNA inserts were excised from plasmid DNA with the appropriate restriction enzymes and purified by agarose gel electrophoresis before labeling with α-[^{32}P]dCTP using a random primer kit (Roche Molecular Biochemicals, Indianapolis, IN). Hybridizations were performed as previously described using a Bellco Autoblot hybridization oven (47). Same blots were reprobed with [^{32}P]-labeled cDNA to *18S* rRNA for loading (48).

AQ: E

Small interfering RNA (siRNA)-MC-4 cells, which contain high levels of *Atf4* mRNA, were seeded at a density of 25,000 cells/cm^2. After 24 h, cells were transfected with mouse *Atf4* siRNA (sense: 5′-GAG CAU UCC UUU AGU UUA GUU-3′; antisense: 5′-CUA AAC UAA AGG AAU GCU CUU-3′) (49) or negative control siRNA (low GC, catalog no. 12935–200; Invitrogen) using LipofectAMINE 2000 (Invitrogen). After 48 h, cells from three identically treated dishes were pooled and harvested for total RNA, followed by quantitative real-time RT-PCR analyses for *Atf4*, *Ocn*, and *Col1(I)* mRNAs. A second set of mouse *Atf4* siRNAs was purchased from Ambion (Austin, TX; catalog no. AM16704, ID 160775 and 160776) and used to confirm the results using the first set of *Atf4* siRNA.

AQ: F

Atf4-deficient mice

Breeding pairs of mice heterozygous for ATF4 (Swiss Black mouse background) were obtained from Dr. Randal J. Kaufman (the Howard

balt3/zee-end/zee-end/zee00408/zee3966-08a | eideg | S=4 | 2/1/08 | 14:49 | Art: EN-07-1573 | Input-ss

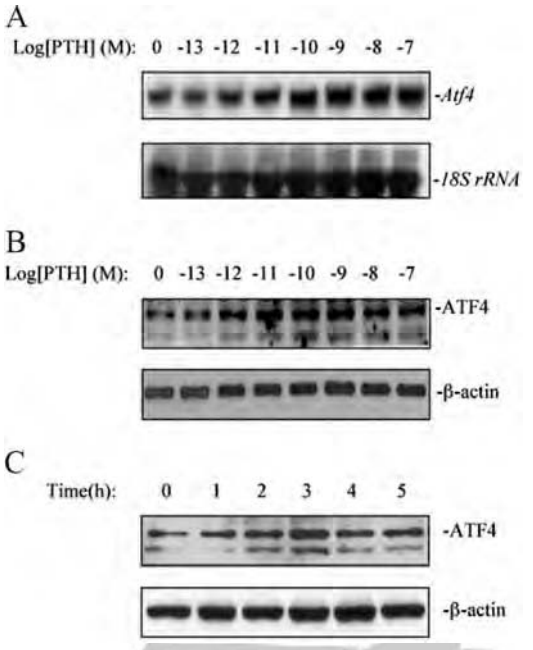

FIG. 1. PTH increases levels of ATF4 expression in osteoblasts. A, Effect of PTH on *Atf4* mRNA. MC-4 cells were seeded at a density of 50,000 cells/cm^2 in 35-mm dishes and cultured in 10% FBS medium overnight. Cells were then treated with various concentration of PTH for 6 h. For each group, total RNA (20 μg/lane) was loaded for Northern hybridization using cDNA probes for mouse *Atf4* mRNA and 18S rRNAs (for normalization). B, Effect of PTH on ATF4 proteins (dose response). MC-4 cells were treated with indicated concentrations of PTH for 6 h and nuclear extracts were prepared for Western blot analysis for ATF4. C, Effect of PTH on ATF4 proteins (time course). MC-4 cells were treated with 10^{-7} M PTH for indicated time (h). Experiments were repeated three to four times, and qualitatively identical results were obtained.

Hughes Medical Institute and the University of Michigan School of Medicine). These mice were originally developed by Dr. Tim M. Townes (University of Alabama at Birmingham) and were used to generate *Atf4* wild-type (*Atf4*$^{+/+}$), heterozygous (*Atf4*$^{+/-}$), and homozygous mutant (*Atf4*$^{-/-}$) embryos/pups for this study. Original reports describing the phenotype of *Atf4* homozygote-null mutants used the identical strain of mice (50). PCR genotyping was performed on tail DNA using a cocktail of three primers (TOWNES-1: 5′-AGC AAA ACA AGA CAG CAG CCA CTA-3′; TOWNES-2: 5′-GTT TCT ACA GCT TCC TCC ACT CTT-3′, and TOWNES-3: 5′-ATA TTG CTG AAG AGC TTG GCGGC-3′) obtained from the laboratories of Dr. Randal J. Kaufman. A 700-bp DNA PCR product was amplified from *Atf4*$^{-/-}$ mouse tail DNA and a 900-bp product from wild-type mice (see Fig. 7A). The genotype of each mouse established by PCR of tail genomic DNA was confirmed by Western blotting of calvaria cell lysates and anti-ATF4 antibody. A breeding colony was established using heterozygote mice to provide littermate controls. All animal studies were approved by the Animal Care Committee of the Veterans Affairs Pittsburgh Healthcare System.

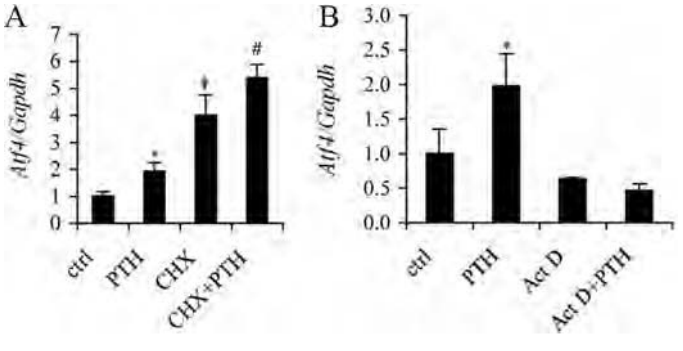

FIG. 2. Effects of CHX/ActD treatment on PTH induction of *Atf4* mRNA. MC-4 cells were treated with vehicle or 10 μg/ml CHX (A) or ActD (B) in the absence or presence of PTH for 6 h. *Atf4* and *Gapdh* mRNAs were determined by quantitative real-time RT-PCR analysis. Experiments were repeated three times, and qualitatively identical results were obtained. *, $P < 0.05$ [control (ctrl) *vs.* PTH]; #, $P < 0.05$ (CHX *vs.* CHX/PTH); ?, $P < 0.05$ (control *vs.* CHX).

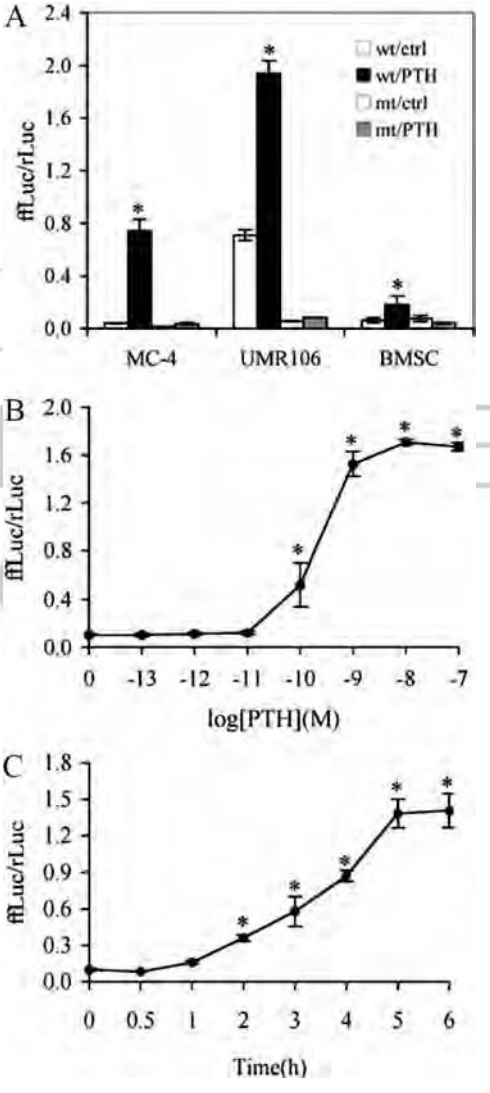

FIG. 3. PTH increases ATF4-dependent transcriptional activity in MC-4 cells. A, Target cell specificity. Cells (MC-4, UMR106–01, and primary BMSCs) were transiently transfected with p4OSE1-luc and renilla luciferase normalization plasmid and treated with 10^{-7} M PTH for 6 h before being harvested and assayed for dual-luciferase activity. Firefly luciferase activity was normalized to renilla luciferase activity (for transfection efficiency). B, Dose dependence. MC-4 cells were transiently transfected as in Fig. 2A and treated with indicated concentration of PTH (from 10^{-11} to 10^{-7} M) for 6 h followed by dual-luciferase assay. C, Time course. MC-4 cells were transiently transfected as in Fig. 2A and treated with 10^{-7} M PTH for indicated times. Data represent mean ± SD. Experiments were repeated three to four times and qualitatively identical results were obtained. *, $P < 0.05$ [control (ctrl) *vs.* PTH].

AQ: I

balt3/zee-end/zee-end/zee00408/zee3966-08a | eideg | S=4 | 2/1/08 | 14:49 | Art: EN-07-1573 | Input-ss

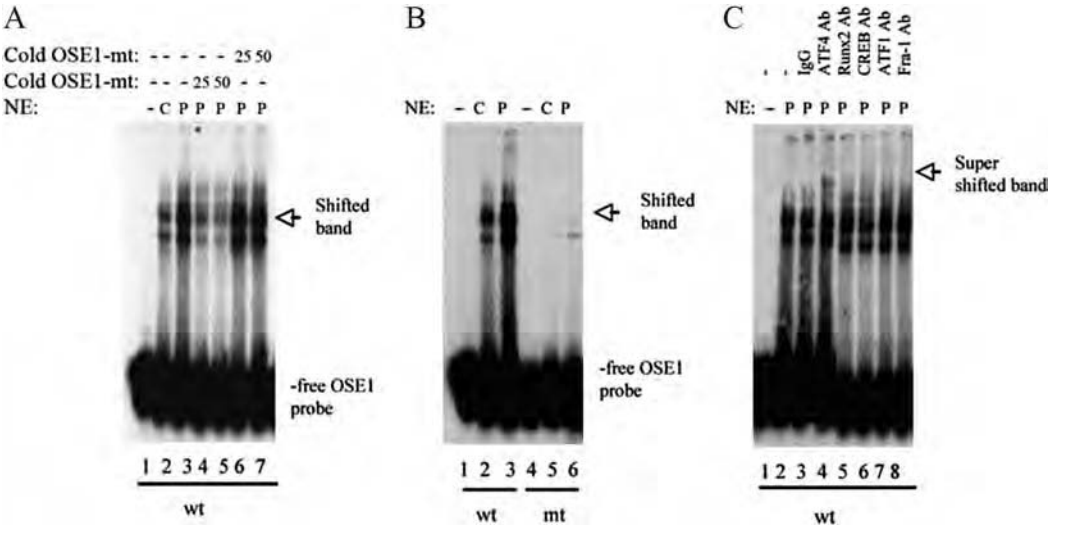

FIG. 4. PTH increases binding of ATF4 to OSE1 DNA. A, PTH increases binding of osteoblast nuclear extracts (NE) to OSE1. Nuclear extracts were prepared from MC-4 cells with (P) (lanes 3–7) or without (C) (lane 2) PTH treatment for 6 h. One microgram of each nuclear extract was incubated with end-labeled double-stranded OSE1 (TGC TTA CAT CAG AGA GCA) and analyzed by electrophoresis on 4% polyacrylamide gels. DNA binding to labeled wild-type OSE1 probe was analyzed in the presence of 25- to 50-fold molar excesses of cold wt (lanes 6 and 7) or mt (lanes 4 and 5) OSE1 (TGC TTA gta CAG AGA GCA) by GMSA using 1 μg of nuclear extracts from PTH-treated MC-4 cells. B, Binding site specificity. Labeled wt (lanes 1–3) and mt (lanes 4–6) OSE1 probes were incubated with 1 μg nuclear extracts from MC-4 cells with and without PTH treatment. C, The nuclear complex binding OSE1 contains ATF4. Labeled wild-type OSE1 probe was incubated with 1 μg nuclear extracts from PTH-treated MC-4 cells in the presence of normal control IgG (lane 3), ATF4 antibody (lane 4), Runx2 antibody (lane 5), CREB antibody (lane 6), ATF1 antibody (lane 7), and Fra-1 antibody (lane 8). Experiments were repeated three to four times, and qualitatively identical results were obtained.

Statistical analysis

Data were analyzed with GraphPad Prism software (GraphPad, San Diego, CA). A one-way ANOVA analysis was used followed by the Dunnett's test (see Fig. 3, B and C). Student's' *t* test was used to test for differences between two groups of data. Differences with a $P < 0.05$ was considered as statistically significant. Results were expressed as means ± SD.

Results

PTH increases ATF4 expression in MC-4 cells

To determine the effect of PTH on *Atf4* mRNA expression, MC-4 cells were treated with increasing concentrations of PTH (from 10^{-13} to 10^{-7} M) for 6 h, and total RNA was isolated for Northern blot analysis. As shown in Fig. 1A, PTH dose-dependently increased levels of *Atf4* mRNAs with a significant stimulatory effect first detected at a concentration of 10^{-10} M. Western blot analyses using nuclear extracts from MC-4 cells with and without PTH treatment show that PTH also dose-dependently elevated the levels of ATF4 protein with maximal stimulation at 10^{-10} M. Measurable stimulation of ATF4 protein was observed 1 h after PTH addition with maximal induction occurring at 3 h and lasting for at least 5 h (Fig. 1, B and C). PTH similarly increased *Atf4* and *Ocn* mRNA expression in mouse primary bone marrow stromal cells (BMSCs) (see Fig. 7, B and C). To assess the molecular mechanisms of PTH stimulation of *Atf4* mRNA expression, MC-4 cells were treated with and without inhibitors of transcription and translation in the presence and absence of PTH (10^{-7} M) for 6 h. As shown in Fig. 2A, the protein synthesis inhibitor CHX alone induced *Atf4* mRNA by 4-fold, which is typically observed in immediate early response genes such as *Fra-2* (15). The PTH-stimulation of *Atf4* mRNA was not blocked by CHX treatment, suggesting that *de novo* protein synthesis is not necessary for the PTH regulation. In contrast, the transcription inhibitor ActD completely abolished the PTH-stimulated *Atf4* mRNA induction (Fig. 2B), suggesting that the PTH effect requires transcription.

PTH increases ATF4-dependent transcriptional activity in osteoblasts

The effect of PTH on ATF4-dependent transcriptional activity was evaluated in two osteoblast cell lines and primary mouse bone marrow stromal cells. Cells were transiently transfected with wt or mt p4OSE1-luc, an artificial promoter containing four copies of wt or mt OSE1 (a specific ATF4-binding element) fused to a −34 to +13 minimal mOG2 promoter, and pRL-SV40, a renilla luciferase normalization plasmid. After 42 h, cells were treated with PTH (10^{-7} M) for 6 h followed by dual-luciferase assay. Firefly luciferase activity was normalized to renilla luciferase activity as a control for transfection efficiency. As shown in Fig. 3A, PTH stimulated ATF4-dependent OSE1 activity by 17-, 2.7-, and 2.8-fold in MC-4, UMR106–01, and primary BMSCs ($P < 0.05$, control *vs.* PTH), respectively. This PTH response was completely lost with the introduction of a 3-bp point mutation in the OSE1 core sequence (from TTA*CAT*CA to TTA*GTA*CA). (Note that there are no additional OSE1 sites in the upstream region of the mOG2 promoter.) Figure 3B shows that PTH stimulated ATF4-dependent transcriptional activity in a dose-dependent manner with a significant stimulatory effect first detected at a concentration of 10^{-10} M. This is consistent with our previous study that examined effects of PTH on endogenous *Ocn* mRNA (33). Time-course studies revealed

balt3/zee-end/zee-end/zee00408/zee3966-08a | eideg | S=4 | 2/1/08 | 14:49 | Art: EN-07-1573 | Input-ss

that the earliest effect of PTH stimulation was seen within 1 h and peaked at 5–6 h (Fig. 3C).

PTH increases ATF4 binding to OSE1 DNA

To determine whether PTH increases ATF4 binding to OSE1 DNA, we performed GMSA using nuclear extracts from MC-4 cells with and without 10^{-7} M PTH for 6 h. Consistent with our previous observation (33), nuclear extracts from PTH-treated MC-4 cells exhibited increased binding to intact OSE1 oligonucleotides (Fig. 4A, lanes 2 and 3), and this binding was significantly reduced by the addition of 25- and 50-fold molar excesses of unlabeled wt OSE1 oligonucleotides (Fig. 4A, lanes 4 and 5) but not by unlabeled mt OSE1 oligonucleotides (Fig. 4A, lane 6 and 7). In contrast, GMSA using labeled mt OSE1 oligonucleotides as probes showed that both basal and PTH-induced binding activity was abolished by the same 3-bp point mutation (Fig. 4B, lanes 4–6). The same mutation also abolished PTH activation of 647- and 116-bp mOG2 promoter fragments and 4OSE1 (33) (Fig. 3A). Importantly, PTH-increased binding to OSE1 was supershifted with an anti-ATF4 antibody (Fig. 4C, lanes 4). In contrast, normal IgG or antibodies against Runx2, CREB, ATF1, and Fra-1 did not significantly supershift the PTH-stimulated band (Fig 4C, lanes 3–8). Taken together, these studies demonstrate that ATF4 is a component of the PTH-stimulated DNA-protein complex associating with OSE1. [Note that PTH treatment did not alter binding of Runx2 to OSE2 DNA in the mOG2 promoter in GMSA (33).]

Protein kinase A (PKA) is the major signaling pathway mediating the PTH response

To identify signaling pathways mediating PTH activation of ATF4 transcriptional activity, we examined the effects of various inhibitors or activators. As shown in Fig. 5A, H89, a selective inhibitor of the PKA pathway, completely abolished PTH-stimulated ATF4 transcriptional activity ($P > 0.05$, control *vs.* PTH). GF109203X, a specific inhibitor of the protein kinase C (PKC) pathway, significantly decreased the PTH stimulation. U0126, a specific inhibitor of MAPK, partially suppressed PTH stimulation. As shown in Fig. 5B, FSK, a well-known activator of PKA, increased ATF4 activity in the absence of PTH in a dose-dependent manner. In combination with PTH, the effect of FSK was not additive, indicating that the PKA pathway was maximally stimulated. PMA, a PKC activator, did not significantly affect the PTH-induced ATF4 activity at a concentration range of 0.1–5 μM. A higher concentration of PMA (20 μM) slightly increased PTH-stimulated ATF4 activity without changing the basal activity (Fig. 5C). Taken together, these results indicate that PKA is the major pathway mediating PTH activation of ATF4 in osteoblasts with PKC and MAPK/ERK pathways playing lesser roles in the PTH response. The concentrations of the inhibitors or activators used in this study are in the range reported to selectively affect the relevant pathways (33, 51–53). We found no evidence of toxicity; compounds did not reduce cell DNA or protein under the current condition (data not shown).

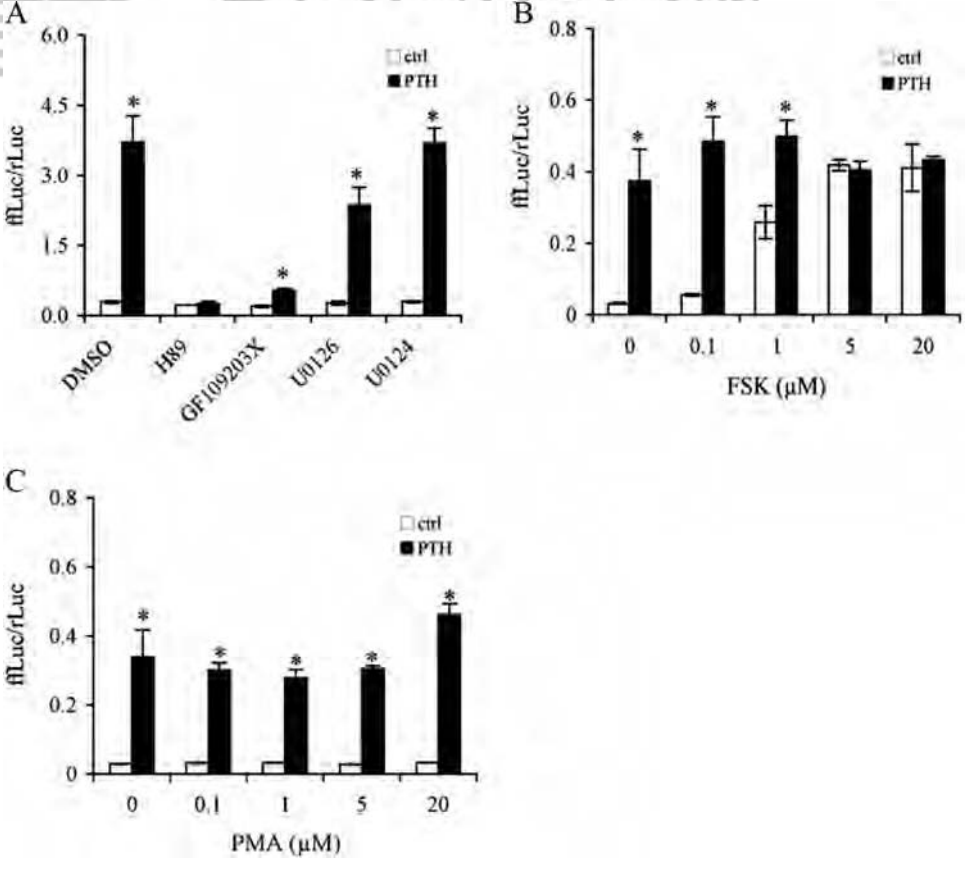

FIG. 5. PKA is the major signaling pathway mediating the PTH response. A, Effects of inhibitors/activators on PTH-induced ATF4 transcriptional activity. MC-4 cells were transiently transfected with p4OSE1-luc and renilla luciferase normalization plasmid. After 42 h, cells were treated with 10 μM inhibitors/activators in the absence or presence of 10^{-7} M PTH for 6 h followed by dual-luciferase assay. Compounds used were: H89, a PKA inhibitor; FSK, a PKA activator; GF109203X, a PKC inhibitor; PMA, a PKC activator; U0126, a MAPK inhibitor; and U0124, an inactive analog of U0126. B and C, Dose-response of FSK (B) and PMA (C) on PTH stimulation of ATF4 transcriptional activity. MC-4 cells were transiently transfected as in Fig. 5A and treated with indicated concentration of respective activator for 6 h in the absence and presence of 10^{-7} M PTH followed by dual-luciferase assay. Data represent mean ± SD. Experiments were repeated three times and qualitatively identical results were obtained. *, $P < 0.05$ [control (ctrl) *vs.* PTH].

balt3/zee-end/zee-end/zee00408/zee3966-08a | eideg | S=4 | 2/1/08 | 14:49 | Art: EN-07-1573 | Input-ss

PTH-dependent induction of Ocn gene expression requires ATF4

We used two separate approaches to establish the requirements for ATF4 in the regulation of *Ocn* gene expression by PTH. First, we examined whether ATF4 is necessary for PTH induction of *Ocn* mRNA expression in osteoblasts by knocking down endogenous *Atf4* transcripts using siRNA. MC-4 cells, which express high levels of *Atf4* mRNA, were transiently transfected with ATF4 siRNA or negative control siRNA (Invitrogen) using LipofectAMINE 2000 according to the manufacturer's instructions. This siRNA specifically targets mouse *Atf4* (49). As shown in Fig. 6A, quantitative real-time RT-PCR analysis showed that ATF4 siRNA (20 and 40 nM) efficiently reduced the levels of *Atf4* mRNA by 57 and 71%, respectively. In contrast, the negative control siRNA did not reduce the *Atf4* mRNA (Fig. 6B). As shown in Fig. 6C, the basal level of *Ocn* mRNA was reduced greater than 70% by ATF4 siRNA ($P < 0.05$, control *vs.* ATF4 siRNA). Importantly, PTH-stimulated *Ocn* mRNA was completely abolished in ATF4 siRNA group relative to the control siRNA group. Conversely, *Col1(I)* mRNA was not altered by ATF4 siRNA or PTH (Fig. 6D). Similar results were obtained when a different set of ATF4 siRNAs was used in MC-4 cells (data not shown).

To further establish the requirement for ATF4 in the PTH response, primary BMSCs were isolated from *wt* and *Atf4*$^{-/-}$ mice (Fig. 7A) and treated with or without PTH (10^{-7} M) for 6 h followed by RNA preparation and quantitative real-time PCR analysis. As shown in Fig. 7B, minimal *Atf4* mRNA was detected by real-time RT/PCR in the *Atf4*$^{-/-}$ BMSCs. Consistent with the results of experiments with MC-4 cells, PTH significantly stimulated *Atf4* mRNA in wt BMSCs ($P < 0.05$, control *vs.* PTH), but this induction was completely lost in cells from *Atf4*$^{-/-}$ mice (Fig. 7B). As shown in Fig. 7C, PTH significantly increased *Ocn* mRNA in wt BMSCs, which was abolished in *Atf4*$^{-/-}$ BMSCs ($P > 0.05$, control *vs.* PTH). The basal level of *Ocn* mRNA was also significantly reduced in *Atf4*$^{-/-}$ BMSCs relative to wt cells ($P < 0.05$, wt *vs.* mt). In contrast, PTH did not increase *Opn* mRNA in wt or mt BMSCs ($P > 0.05$, control *vs.* PTH) (Fig. 7D). However, the level of *Opn* mRNA was increased in *Atf4*$^{-/-}$ cells ($P < 0.05$, wt *vs.* mt), indicating that ATF4 may function as a negative regulator of *Opn* expression (Fig. 7D). In addition, the levels of *Pth1r* mRNA were not significantly changed by either ATF4 deficiency or PTH, suggesting that PTH signaling is intact in the absence of ATF4 (Fig. 7E). Taken together, these data clearly establish that ATF4 is required for PTH induction of *Ocn* mRNA in primary BMSCs.

Discussion

This study examined actions of PTH on ATF4 expression and activity in osteoblasts. Using the *Ocn* gene as a model system for studying PTH-dependent transcription, we found the following: 1) PTH rapidly induces *Atf4* expression in MC-4 cells and mouse primary bone marrow stromal cells in a time- and dose-dependent manners; 2) PTH increases *in vitro* binding of ATF4 to OSE1 DNA; 3) PTH dramatically activates ATF4 transcriptional activity mainly through the PKA pathway; 4) PTH stimulation of *Ocn* gene expression requires ATF4 because it is abolished by ATF4 siRNA in MC-4 cells and is not seen in ATF4-deficeint BMSCs. Col-

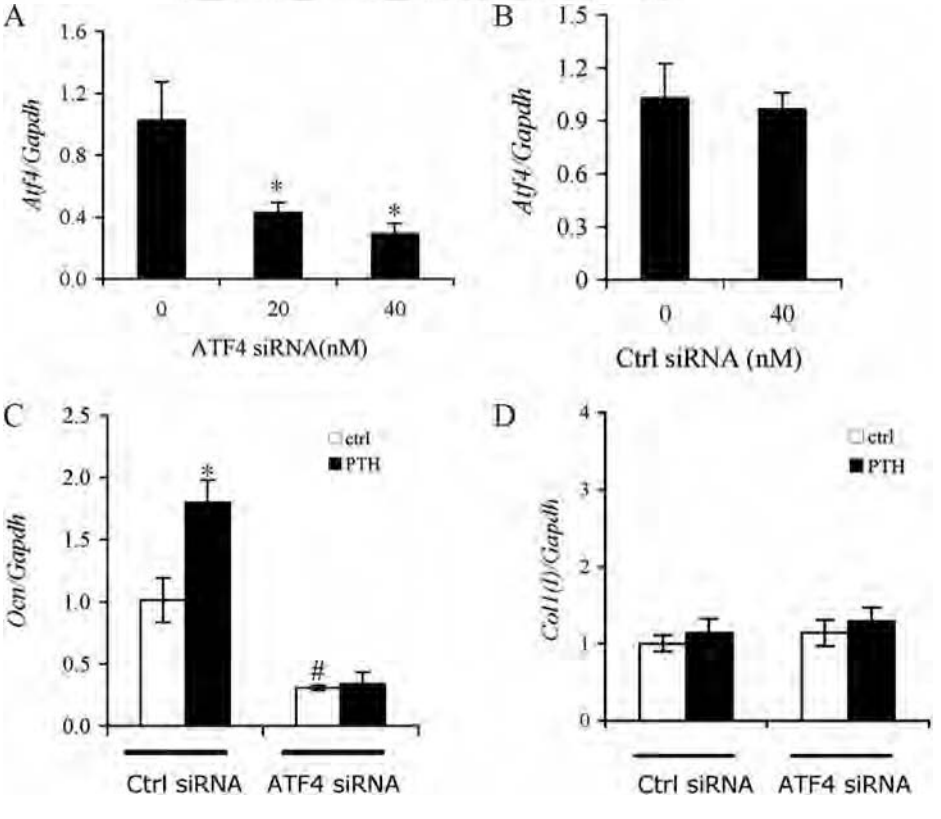

FIG. 6. ATF4 siRNA blocks PTH stimulation of *Ocn* expression. A and B, MC-4 cells were transiently transfected with *Atf4* siRNA (A) or negative control (Ctrl) siRNA (B). After 48 h, total RNA was prepared for quantitative real-time RT-PCR analyses for *Atf4* mRNA, which was normalized to *Gapdh* mRNA. C and D, MC-4 cells were transiently transfected with 40 nM *Atf4* siRNA or negative control siRNAs. After 42 h, cells were treated with and without 10^{-7} M PTH for 6 h followed by RNA preparation and quantitative real-time RT-PCR analyses for *Ocn* and *Col1(I)* mRNAs, which were normalized to the *Gapdh* mRNAs. *, $P < 0.05$ (ctrl *vs.* PTH); #, $P < 0.05$ (ctrl siRNA *vs.* ATF4 siRNA). Data represent mean ± SD. Experiments were repeated three times, and qualitatively identical results were obtained.

balt3/zee-end/zee-end/zee00408/zee3966-08a | eideg | S=4 | 2/1/08 | 14:49 | Art: EN-07-1573 | Input-ss

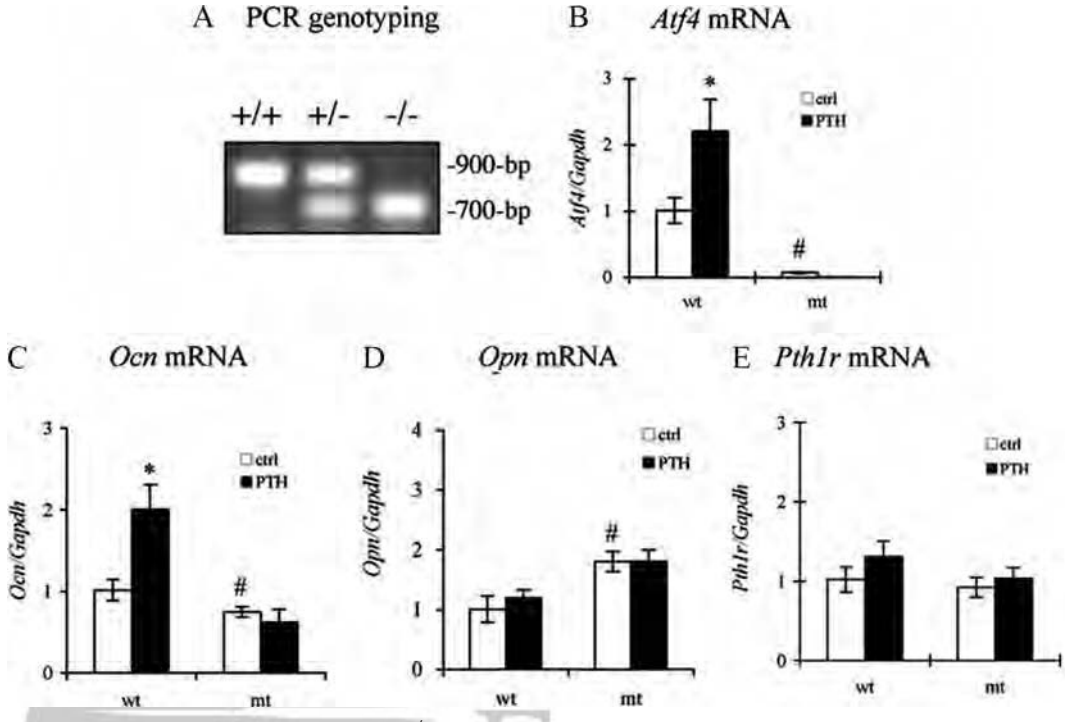

FIG. 7. PTH stimulation of *Ocn* expression is lost in $Atf4^{-/-}$ BMSCs. A, PCR genotyping was performed on tail DNA using a cocktail of three primers (see *Materials and Methods*). A 700-bp DNA PCR product is amplified from $Atf4^{-/-}$ mouse tail DNA and a 900-bp product from wild-type mice. B–E, Effects of ATF4 deficiency on PTH stimulation of *Atf4* (B), *Ocn* (C), *Opn* (D), and *Pth1r* (E) expression in BMSCs. Primary BMSCs were seeded at a density of 50,000 cells/cm^2 in 35-mm dishes and cultured in 10% FBS medium overnight. Cells were then treated with 10^{-7} M PTH for 6 h followed by RNA preparation and quantitative real-time RT/PCR for *Atf4* (B), *Ocn* (C), *Opn* (D), and *Pth1r* (E) mRNA, which were normalized to the *Gapdh* mRNAs. *, $P < 0.05$ (ctrl *vs.* PTH); #, $P < 0.05$ (wt *vs.* mt). Data represent mean ± SD. Experiments were repeated three times, and qualitatively identical results were obtained.

lectively, this study establishes that ATF4 is a novel downstream target of PTH actions in osteoblasts.

It is well documented that PTH signals mainly through the PKA pathway. In the present study, we show that PKA inhibition completely blocked PTH stimulation of ATF4 activity. Furthermore, activation of the PKA pathway by FSK dramatically increased ATF4 activity in the absence of PTH. However, when combined with PTH, the effect of FSK was not additive. These results strongly suggest that PKA is the major pathway for PTH to activate ATF4 because each agent (*i.e.* FSK or PTH) maximally stimulates the same pathway, making additional ATF4 activation impossible. Inhibition of the PKC pathway also resulted in a significant reduction in PTH-induced ATF4 activity (data not shown), but PKC activation by PMA failed to activate both basal or PTH-induced ATF4 activity. Thus, PKC is partially required for PTH activation of ATF4. Lastly, inhibition of the MAPK/ERK pathway led to partial inhibition of the PTH stimulation. These three pathways are also required for PTH induction of both *Ocn* mRNA and 1.3-kb *mOG2* promoter activity as previously described (33), further supporting our hypothesis that ATF4 mediates PTH induction of *Ocn* gene expression.

A recent study showed that ATF4 mediates β-adrenergic induction of *Rankl* mRNA expression via direct binding to the upstream OSE1 site in the *Rankl* promoter in osteoblasts (54). However, PTH stimulation of *Rankl* expression was not reduced in the absence of ATF4, suggesting that this catabolic action of PTH is independent of this transcription factor. Phosphorylation seems to be critical for ATF4 to elicit its function in osteoblasts and bone. A PKA phosphorylation site (serine 254) within the ATF4 molecule was recently shown to mediate β-adrenergic induction of *Rankl* mRNA expression in osteoblasts (54). In addition, ATF4 is phosphorylated at serine 251 by ribosomal kinase 2 (RSK2), the kinase inactivated in Coffin-Lowry syndrome, an X-linked mental retardation disorder associated with skeletal manifestations (29). Because RSK2 is an immediate downstream target of MAPK/ERK that is activated by PTH signaling (8, 9), PTH may in part activate ATF4 via the MAPK/ERK/RSK2 pathway. It remains to be determined whether the PKA and/or RSK2 phosphorylation sites are involved in the PTH activation of ATF4.

One of the major downstream factors for PTH signaling is CREB, the cAMP response element binding protein. Actions of CREB are mediated through cAMP response elements (CREs) in the regulatory regions of target genes. PTH phosphorylates CREB at serine 133. This phosphorylation event stimulates the binding of CREB to the CRE and is required for CREB to activate transcription of target genes. Through this classical pathway, PTH rapidly induces transcription of immediate-early response genes including those encoding activator protein-1 family members such as c-Fos, c-Jun, Fra-1, Fra-2, and FosB (10, 14, 15, 52, 55–57). Although CREB was shown to binding to the OSE1 site (29), overexpression of CREB was unable to activate OSE1-dependent transcription activity of the mOG2 promoter *in vitro* (29), suggesting

balt3/zee-end/zee-end/zee00408/zee3966-08a | eideg | S=4 | 2/1/08 | 14:49 | Art: EN-07-1573 | Input-ss

that this site is not a major functional site for CREB. Furthermore, the OSE1 binding activity stimulated by PTH was not supershifted by an anti-CREB antibody. Instead, this complex clearly contains ATF4 protein (Fig. 4C). Thus, we were unable to obtain any evidence for the involvement of CREB in the PTH response. However, our results do not exclude the possibility that PTH/CREB activates *Atf4* mRNA transcription via CREB binding to potential CRE sites in the *Atf4* promoter.

PTH induction of immediate-early response genes occurs very rapidly (minutes to hours) and lasts for several hours. This PTH response is usually independent upon the presence of *de novo* protein synthesis but requires active cellular transcription. The time-course experiments in the present study indicate that PTH induction of *Atf4* occurs within 1 h of PTH addition and peaks after 3–6 h. Furthermore, this regulation depends on active cellular transcription and does not require *de novo* protein synthesis. Therefore, ATF4 may be considered as an additional PTH early response gene.

ATF4-deficeint mice as well as humans with mutations in RSK2, an ATF4 activating kinase, exhibit striking deficits in bone formation and osteoblast activity. Because ATF4 is required for osteoblast function and bone formation *in vivo*, and as shown herein, ATF4 is a novel downstream target of PTH in osteoblasts, it will be important to determine whether ATF4 is also required for the anabolic actions of PTH in bone.

Acknowledgments

We thank Dr. Randal J. Kaufman (Howard Hughes Medical Institute and the University of Michigan School of Medicine) for providing us with the *Atf4*-deficient mice.

Received November 15, 2007. Accepted December 31, 2007.

Address all correspondence and requests for reprints to: Dr. Guozhi Xiao, Division of Hematology/Oncology, Department of Medicine, University of Pittsburgh; Veterans Affairs Pittsburgh Healthcare System, Research and Development, 151-U, Room 2W-111, University Drive C, Pittsburgh, Pennsylvania 15240. E-mail: xiaog@upmc.edu.

This work was supported by National Institutes of Health Grants DK072230 (to G.X.) and DE11723 and DE12211 (to R.T.F.) and Department of Defense Grant W81XWH-07–1-0160 (to G.X.)

Disclosure Statement: The authors of this manuscript have nothing to disclose.

References

1. **Neer RM, Arnaud CD, Zanchetta JR, Prince R, Gaich GA, Reginster JY, Hodsman AB, Eriksen EF, Ish-Shalom S, Genant HK, Wang O, Mitlak BH** 2001 Effect of parathyroid hormone (1–34) on fractures and bone mineral density in postmenopausal women with osteoporosis. N Engl J Med 344:1434–1441
2. **Miao D, He B, Karaplis AC, Goltzman D** 2002 Parathyroid hormone is essential for normal fetal bone formation. J Clin Invest 109:1173–1182
3. **Demiralp B, Chen HL, Koh AJ, Keller ET, McCauley LK** 2002 Anabolic actions of parathyroid hormone during bone growth are dependent on c-*fos*. Endocrinology 143:4038–4047
4. **Partridge NC, Alcorn D, Michelangeli VP, Kemp BE, Ryan GB, Martin TJ** 1981 Functional properties of hormonally responsive cultured normal and malignant rat osteoblastic cells. Endocrinology 108:213–219
5. **McCauley LK, Koh AJ, Beecher CA, Cui Y, Decker JD, Franceschi RT** 1995 Effects of differentiation and transforming growth factor β1 on PTH/PTHrP receptor mRNA levels in MC3T3–E1 cells. J Bone Miner Res 10:1243–1255
6. **McCauley LK, Koh AJ, Beecher CA, Cui Y, Rosol TJ, Franceschi RT** 1996 PTH/PTHrP receptor is temporally regulated during osteoblast differentiation and is associated with collagen synthesis. J Cell Biochem 61:638–647
7. **Swarthout JT, D'Alonzo RC, Selvamurugan N, Partridge NC** 2002 Parathyroid hormone-dependent signaling pathways regulating genes in bone cells. Gene 282:1–17
8. **Carpio L, Gladu J, Goltzman D, Rabbani SA** 2001 Induction of osteoblast differentiation indexes by PTHrP in MG-63 cells involves multiple signaling pathways. Am J Physiol Endocrinol Metab 281:E489–E499
9. **Swarthout JT, Doggett TA, Lemker JL, Partridge NC** 2001 Stimulation of extracellular signal-regulated kinases and proliferation in rat osteoblastic cells by parathyroid hormone is protein kinase C-dependent. J Biol Chem 276:7586–7592
10. **Pearman AT, Chou WY, Bergman KD, Pulumati MR, Partridge NC** 1996 Parathyroid hormone induces c-*fos* promoter activity in osteoblastic cells through phosphorylated cAMP response element (CRE)-binding protein binding to the major CRE. J Biol Chem 271:25715–25721
11. **Gonzalez GA, Montminy MR** 1989 Cyclic AMP stimulates somatostatin gene transcription by phosphorylation of CREB at serine 133. Cell 59:675–680
12. **Selvamurugan N, Chou WY, Pearman AT, Pulumati MR, Partridge NC** 1998 Parathyroid hormone regulates the rat collagenase-3 promoter in osteoblastic cells through the cooperative interaction of the activator protein-1 site and the runt domain binding sequence. J Biol Chem 273:10647–10657
13. **D'Alonzo RC, Kowalski AJ, Denhardt DT, Nickols GA, Partridge NC** 2002 Regulation of collagenase-3 and osteocalcin gene expression by collagen and osteopontin in differentiating MC3T3–E1 cells. J Biol Chem 277:24788–24798
14. **McCauley LK, Koh AJ, Beecher CA, Rosol TJ** 1997 Proto-oncogene c-*fos* is transcriptionally regulated by parathyroid hormone (PTH) and PTH-related protein in a cyclic adenosine monophosphate-dependent manner in osteoblastic cells. Endocrinology 138:5427–5433
15. **McCauley LK, Koh-Paige AJ, Chen H, Chen C, Ontiveros C, Irwin R, McCabe LR** 2001 Parathyroid hormone stimulates fra-2 expression in osteoblastic cells *in vitro* and *in vivo*. Endocrinology 142:1975–1981
16. **Ogata Y, Nakao S, Kim RH, Li JJ, Furuyama S, Sugiya H, Sodek J** 2000 Parathyroid hormone regulation of bone sialoprotein (BSP) gene transcription is mediated through a pituitary-specific transcription factor-1 (Pit-1) motif in the rat BSP gene promoter. Matrix Biol 19:395–407
17. **Krishnan V, Moore TL, Ma YL, Helvering LM, Frolik CA, Valasek KM, Ducy P, Geiser AG** 2003 Parathyroid hormone bone anabolic action requires cbfa1/runx2-dependent signaling. Mol Endocrinol 17:423–435
18. **Ducy P, Zhang R, Geoffroy V, Ridall AL, Karsenty G** 1997 Osf2/Cbfa1: a transcriptional activator of osteoblast differentiation. Cell 89:747–754
19. **Ducy P, Karsenty G** 1995 Two distinct osteoblast-specific *cis*-acting elements control expression of a mouse osteocalcin gene. Mol Cell Biol 15:1858–1869
20. **Merriman HL, van Wijnen AJ, Hiebert S, Bidwell JP, Fey E, Lian J, Stein J, Stein GS** 1995 The tissue-specific nuclear matrix protein, NMP-2, is a member of the AML/CBF/PEBP2/runt domain transcription factor family: interactions with the osteocalcin gene promoter. Biochemistry 34:13125–13132
21. **Stein GS, Lian JB, van Wijnen AJ, Stein JL** 1997 The osteocalcin gene: a model for multiple parameters of skeletal-specific transcriptional control. Mol Biol Rep 24:185–196
22. **Banerjee C, McCabe LR, Choi JY, Hiebert SW, Stein JL, Stein GS, Lian JB** 1997 Runt homology domain proteins in osteoblast differentiation: AML3/CBFA1 is a major component of a bone-specific complex. J Cell Biochem 66:1–8
23. **Banerjee C, Hiebert SW, Stein JL, Lian JB, Stein GS** 1996 An AML-1 consensus sequence binds an osteoblast-specific complex and transcriptionally activates the osteocalcin gene. Proc Natl Acad Sci USA 93:4968–4973
24. **Lian JB, Stein GS** 2003 Runx2/Cbfa1: a multifunctional regulator of bone formation. Curr Pharm Des 9:2677–2685
25. **Xiao G, Jiang D, Ge C, Zhao Z, Lai Y, Boules H, Phimphilai M, Yang X, Karsenty G, Franceschi RT** 2005 Cooperative Interactions between activating transcription factor 4 and Runx2/Cbfa1 stimulate osteoblast-specific osteocalcin gene expression. J Biol Chem 280:30689–30696
26. **Stein GS, Lian JB, Stein JL, van Wijnen AJ, Frankel B, Montecino M** 1996 Mechanisms regulating osteoblast proliferation and differentiation. In: JP Bilezikian LGR, Rodon GA, ed. Principles of bone biology. San Diego: Academic Press; 69–86 **AQ: H**
27. **Lian JB, Stein GS, Stein JL, Van Wijnen A, McCabe L, Banerjee C, Hoffmann H** 1996 The osteocalcin gene promoter provides a molecular blueprint for regulatory mechanisms controlling bone tissue formation: role of transcription factors involved in development. Connect Tissue Res 35:15–21
28. **Ducy P, Karsenty, G** 1999 Transcriptional control of osteoblast differentiation. Endocrinologist 9:32–35
29. **Yang X, Matsuda K, Bialek P, Jacquot S, Masuoka HC, Schinke T, Li L, Brancorsini S, Sassone-Corsi P, Townes TM, Hanauer A, Karsenty G** 2004 ATF4 Is a substrate of RSK2 and an essential regulator of osteoblast biology: implication for Coffin-Lowry syndrome. Cell 117:387–398
30. **Boguslawski G, Hale LV, Yu XP, Miles RR, Onyia JE, Santerre RF, Chandrasekhar S** 2000 Activation of osteocalcin transcription involves interaction of protein kinase A- and protein kinase C-dependent pathways. J Biol Chem 275:999–1006
31. **Yu XP, Chandrasekhar S** 1997 Parathyroid hormone (PTH 1–34) regulation of rat osteocalcin gene transcription. Endocrinology 138:3085–3092
32. **Boudreaux JM, Towler DA** 1996 Synergistic induction of osteocalcin gene expression: identification of a bipartite element conferring fibroblast growth factor 2 and cyclic AMP responsiveness in the rat osteocalcin promoter. J Biol Chem 271:7508–7515
33. **Jiang D, Franceschi RT, Boules H, Xiao G** 2004 Parathyroid hormone induction of the osteocalcin gene: requirement for an osteoblast-specific element 1

sequence in the promoter and involvement of multiple signaling pathways. J Biol Chem 279:5329–5337
34. **Yang X, Karsenty G** 2004 ATF4, the osteoblast accumulation of which is determined post-translationally, can induce osteoblast-specific gene expression in non-osteoblastic cells. J Biol Chem 279:47109–47114
35. **Karpinski BA, Morle GD, Huggenvik J, Uhler MD, Leiden JM** 1992 Molecular cloning of human CREB-2: an ATF/CREB transcription factor that can negatively regulate transcription from the cAMP response element. Proc Natl Acad Sci USA 89:4820–4824
36. **Tsujimoto A, Nyunoya H, Morita T, Sato T, Shimotohno K** 1991 Isolation of cDNAs for DNA-binding proteins which specifically bind to a tax-responsive enhancer element in the long terminal repeat of human T-cell leukemia virus type I. J Virol 65:1420–1426
37. **Brindle PK, Montminy MR** 1992 The CREB family of transcription activators. Curr Opin Genet Dev 2:199–204
38. **Hai T, Wolfgang CD, Marsee DK, Allen AE, Sivaprasad U** 1999 ATF3 and stress responses. Gene Expr 7:321–335
39. **Meyer TE, Habener JF** 1993 Cyclic adenosine 3′,5′-monophosphate response element binding protein (CREB) and related transcription-activating deoxyribonucleic acid-binding proteins. Endocr Rev 14:269–290
40. **Sassone-Corsi P** 1994 Goals for signal transduction pathways: linking up with transcriptional regulation. EMBO J 13:4717–4728
41. **Ziff EB** 1990 Transcription factors: a new family gathers at the cAMP response site. Trends Genet 6:69–72
42. **Yu VW, Ambartsoumian G, Verlinden L, Moir JM, Prud'homme J, Gauthier C, Roughley PJ, St. Arnaud R** 2005 FIAT represses ATF4-mediated transcription to regulate bone mass in transgenic mice. J Cell Biol 169:591–601
43. **Xiao G, Cui Y, Ducy P, Karsenty G, Franceschi RT** 1997 Ascorbic acid-dependent activation of the osteocalcin promoter in MC3T3–E1 preosteoblasts: requirement for collagen matrix synthesis and the presence of an intact OSE2 sequence. Mol Endocrinol 11:1103–1113
44. **Wang D, Christensen K, Chawla K, Xiao G, Krebsbach PH, Franceschi RT** 1999 Isolation and characterization of MC3T3–E1 preosteoblast subclones with distinct *in vitro* and *in vivo* differentiation/mineralization potential. J Bone Miner Res 14:893–903
45. **Benson MD, Bargeon JL, Xiao G, Thomas PE, Kim A, Cui Y, Franceschi RT** 2000 Identification of a homeodomain binding element in the bone sialoprotein gene promoter that is required for its osteoblast-selective expression. J Biol Chem 275:13907–13917
46. **Wang J, Xi L, Hunt JL, Gooding W, Whiteside TL, Chen Z, Godfrey TE, Ferris RL** 2004 Expression pattern of chemokine receptor 6 (CCR6) and CCR7 in squamous cell carcinoma of the head and neck identifies a novel metastatic phenotype. Cancer Res 64:1861–1866
47. **Franceschi RT, Iyer BS, Cui Y** 1994 Effects of ascorbic acid on collagen matrix formation and osteoblast differentiation in murine MC3T3–E1 cells. J Bone Miner Res 9:843–854
48. **Renkawitz R, Gerbi SA, Glatzer KH** 1979 Ribosomal DNA of fly *Sciara coprophila* has a very small and homogeneous repeat unit. Mol Gen Genet 173:1–13
49. **Adams CM** 2007 Role of the transcription factor ATF4 in the anabolic actions of insulin and the anti-anabolic actions of glucocorticoids. J Biol Chem 282:16744–16753
50. **Masuoka HC, Townes TM** 2002 Targeted disruption of the activating transcription factor 4 gene results in severe fetal anemia in mice. Blood 99:736–745
51. **Xiao G, Gopalakrishnan R, Jiang D, Reith E, Benson MD, Franceschi RT** 2002 Bone morphogenetic proteins, extracellular matrix, and mitogen-activated protein kinase signaling pathways are required for osteoblast-specific gene expression and differentiation in MC3T3–E1 cells. J Bone Miner Res 17:101–110
52. **Selvamurugan N, Pulumati MR, Tyson DR, Partridge NC** 2000 Parathyroid hormone regulation of the rat collagenase-3 promoter by protein kinase A-dependent transactivation of core binding factor α1. J Biol Chem 275:5037–5042
53. **Ouyang H, Franceschi R, McCauley L, Wang D, Somerman M** 2000 Parathyroid hormone-related protein downregulates bone sialoprotein gene expression in cementoblasts: role of the protein kinase A pathway. Endocrinology 141:4671–4680
54. **Elefteriou F, Ahn JD, Takeda S, Starbuck M, Yang X, Liu X, Kondo H, Richards WG, Bannon TW, Noda M, Clement K, Vaisse C, Karsenty G** 2005 Leptin regulation of bone resorption by the sympathetic nervous system and CART. Nature 434:514–520
55. **Porte D, Tuckermann J, Becker M, Baumann B, Teurich S, Higgins T, Owen MJ, Schorpp-Kistner M, Angel P** 1999 Both AP-1 and Cbfa1-like factors are required for the induction of interstitial collagenase by parathyroid hormone. Oncogene 18:667–678
56. **Tyson DR, Swarthout JT, Partridge NC** 1999 Increased osteoblastic c-*fos* expression by parathyroid hormone requires protein kinase A phosphorylation of the cyclic adenosine 3′,5′-monophosphate response element-binding protein at serine 133. Endocrinology 140:1255–1261
57. **Koe RC, Clohisy JC, Tyson DR, Pulumati MR, Cook TF, Partridge NC** 1997 Parathyroid hormone versus phorbol ester stimulation of activator protein-1 gene family members in rat osteosarcoma cells. Calcif Tissue Int 61:52–58

***Endocrinology* is published monthly by The Endocrine Society (http://www.endo-society.org), the foremost professional society serving the endocrine community.**

Supplemental Material can be found at:
http://www.jbc.org/cgi/content/full/M705653200/DC1

P2

THE JOURNAL OF BIOLOGICAL CHEMISTRY VOL. 283, NO. 9, pp. 5542–5553, February 29, 2008
© 2008 by The American Society for Biochemistry and Molecular Biology, Inc. Printed in the U.S.A.

General Transcription Factor IIA-γ Increases Osteoblast-specific *Osteocalcin* Gene Expression via Activating Transcription Factor 4 and Runt-related Transcription Factor 2*[S]

Received for publication, July 10, 2007, and in revised form, December 31, 2007 Published, JBC Papers in Press, January 2, 2008, DOI 10.1074/jbc.M705653200

Shibing Yu[‡], Yu Jiang[§], Deborah L. Galson[‡], Min Luo[‡], Yumei Lai[‡], Yi Lu[‡], Hong-Jiao Ouyang[‡], Jian Zhang[‡], and Guozhi Xiao[‡1]

From the Departments of [‡]Medicine and [§]Pharmacology, University of Pittsburgh, Pittsburgh, Pennsylvania 15240

ATF4 (activating transcription factor 4) is an osteoblast-enriched transcription factor that regulates terminal osteoblast differentiation and bone formation. ATF4 knock-out mice have reduced bone mass (severe osteoporosis) throughout life. Runx2 (runt-related transcription factor 2) is a runt domain-containing transcription factor that is essential for bone formation during embryogenesis and postnatal life. In this study, we identified general transcription factor IIAγ (TFIIAγ) as a Runx2-interacting factor in a yeast two-hybrid screen. Immunoprecipitation assays confirmed that TFIIAγ interacts with Runx2 in osteoblasts and when coexpressed in COS-7 cells or using purified glutathione *S*-transferase fusion proteins. Chromatin immunoprecipitation assay of MC3T3-E1 (clone MC-4) preosteoblast cells showed that in intact cells TFIIAγ is recruited to the region of the *osteocalcin* promoter previously shown to bind Runx2 and ATF4. A small region of Runx2 (amino acids 258–286) was found to be required for TFIIAγ binding. Although TFIIAγ interacts with Runx2, it does not activate Runx2. Instead, TFIIAγ binds to and activates ATF4. Furthermore, TFIIAγ together with ATF4 and Runx2 stimulates *osteocalcin* promoter activity and endogenous mRNA expression. Small interfering RNA silencing of *TFIIAγ* markedly reduces levels of endogenous ATF4 protein and *Ocn* mRNA in osteoblastic cells. Overexpression of TFIIAγ increases levels of ATF4 protein. Finally, TFIIAγ significantly prevents ATF4 degradation. This study shows that a general transcription factor, TFIIAγ, facilitates osteoblast-specific gene expression through interactions with two important bone transcription factors ATF4 and Runx2.

Skeletal integrity requires a balance between bone-forming cells (osteoblasts) and bone-resorbing cells or osteoclasts. Imbalance between bone formation and resorption results in metabolic bone diseases such as osteoporosis. Multipotential mesenchymal cells proliferate and differentiate into osteoblasts that synthesize and deposit the mineralizing extracellular matrix of bone. Osteoblast activity is regulated by a number of growth factors and hormones, including bone morphogenetic proteins, insulin-like growth factor 1, basic fibroblast growth factor 2, parathyroid hormone, tumor necrosis factor-α, and extracellular matrix signals (1–9). Runx2 is a runt domain-containing transcription factor identified as a transcriptional activator of osteoblast differentiation and the master gene for bone development *in vitro* and *in vivo* (10–14). Runx2 knock-out mice die at birth and completely lack both skeletal ossification and mature osteoblasts (10, 12). Runx2 haplo-insufficiency causes the skeletal disorder, cleidocranial dysplasia, a disease characterized by defective endochondral and intramembranous bone formation. Runx2 is expressed in mesenchymal condensations during early development at E11.5 and acts as an osteoblast differentiation factor (13).

ATF4 (activating transcription factor 4), also known as CREB2 (cAMP-response element-binding protein 2) (15) and Tax-responsive Enhancer Element B67 (TAXREB67) (16), is a member of the activating transcription factor cAMP-response element-binding protein family of leucine zipper factors that also includes cAMP-response element-binding protein, cAMP-response element modulator (CREM)[2] ATF1, ATF2, ATF3, and ATF4 (17–21). These proteins bind to DNA via their basic region and dimerize via their leucine domain to form a large variety of homodimers and/or heterodimers that allow the cell to coordinate signals from multiple pathways (17–21). An *in vivo* role for ATF4 in bone development was established using *Atf4*-deficient mice (22). ATF4 is required for expression of *osteocalcin* (*Ocn*) and *bone sialoprotein* (*Bsp*) as demonstrated by a dramatic reduction of their mRNAs in $Atf4^{-/-}$ bone (22). ATF4 activates *Ocn* transcription through direct binding to the OSE1 site of the *mOG2* promoter. In addition, ATF4 interacts with Runx2 in osteoblasts or when coexpressed in COS-7 cells. ATF4 and Runx2 cooperatively regulate *Ocn* transcription through interactions with OSE1 (osteoblast-specific element 1)

* This work was supported by National Institutes of Health Grant DK072230 and Department of Defense Grant W81XWH-07-1-0160 (to G. X.). The costs of publication of this article were defrayed in part by the payment of page charges. This article must therefore be hereby marked "*advertisement*" in accordance with 18 U.S.C. Section 1734 solely to indicate this fact.

[S] The on-line version of this article (available at http://www.jbc.org) contains supplemental Figs. S1 and S2.

[1] To whom correspondence should be addressed: Division of Hematology/Oncology, Dept of Medicine, University of Pittsburgh, Veterans Affairs Pittsburgh Healthcare System, Research and Development, 151-U, Rm. 2W-111, University Dr. C, Pittsburgh, PA 15240. Tel.: 412-688-6000 (Ext. 814459); Fax: 412- 688-6960; E-mail: xiaog@upmc.edu.

[2] The abbreviations used are: CREM, cAMP-response element modulator; TFIIAγ, transcription factor IIAγ; ChIP, chromatin immunoprecipitation; GST, glutathione *S*-transferase; WB, Western blot; IP, immunoprecipitation; FBS, fetal bovine serum; RT, reverse transcription; siRNA, small interfering RNA; aa, amino acids; CHX, cycloheximide; VDR, vitamin D receptor.

Downloaded from www.jbc.org at University of Pittsburgh on July 4, 2008

and OSE2 (osteoblast-specific element 2, also known as nuclear matrix protein 2 or NMP2-binding site) sites in the promoter (23–25).

One of the most striking characteristics of ATF4 protein is its very short half-life (30–60 min) in many cell types (26). ATF4 is rapidly degraded via a ubiquitin/proteasomal pathway. This degradation requires the presence of the serine residue 219 in the context of DSG*XXX*S within the ATF4 molecule and its phosphorylation by an unknown kinase. This phosphorylation was shown to be required for subsequent recognition by the $SCF^{\beta TrCP}$ and degradation by the 26 S proteasome (27). Although *Atf4* mRNA is ubiquitously expressed, ATF4 protein preferentially accumulates in osteoblasts (28). This accumulation is explained by a selective reduction of proteasomal degradation in osteoblasts. Indeed, inhibition of the ubiquitin/proteasomal pathway by MG115, which blocks the N-terminal threonine in the active site of β-subunit of 26 S proteasomal complex (29, 30), led to ATF4 accumulation and induced *Ocn* mRNA expression in non-osteoblastic cells (28). These observations suggest that modulation of ATF4 stability constitutes an important step to control its protein level and activity and, ultimately, osteoblast-specific gene expression and bone formation.

Transcription factor IIA (TFIIA) is a general transcription factor consisting of three subunits designated TFIIAα, TFIIAβ, and TFIIAγ (31). TFIIA interacts with and stabilizes TFIID (also known as TBP, TATA box-binding protein) to DNA and activates transcription (32, 33). Although TFIIA was classified as a general transcription factor when it was first identified, more and more evidence shows that this elusive factor may play an important role in the regulation of tissue-specific gene expression via interactions with tissue- or cell type-specific transcription factors (34–36).

The *Ocn* promoter has been the major paradigm for unraveling the mechanisms mediating osteoblast-specific gene expression and defining a number of key transcription factors or cofactors (13, 14, 23–25, 37–41). However, very few studies have focused on how tissue-specific transcription factors interface with general transcriptional initiation factors in osteoblasts. In this study, by using a combination of a yeast two-hybrid system and pulldown assays as well as functional assays, we show that TFIIAγ, the smallest subunit (12 kDa) of TFIIA (42), interacts with both Runx2 and ATF4. TFIIAγ delays ATF4 protein degradation and increases its activity. Together with ATF4 and Runx2, TFIIAγ enhances osteoblast-specific *Ocn* gene expression.

EXPERIMENTAL PROCEDURES

Reagents—Tissue culture media were purchased from Invitrogen and fetal bovine serum from HyClone (Logan, UT). Other reagents were obtained from the following sources: antibodies against TFIIA-α, TFIIA-γ, ATF4, Runx2, and horseradish peroxidase-conjugated mouse or goat IgG from Santa Cruz Biotechnology (Santa Cruz, CA), mouse monoclonal antibody against β-actin from Sigma, and GST antibody from Amersham Biosciences. All other chemicals were of analytical grade.

Cell Cultures—Mouse MC3T3-E1 subclone 4 (MC-4) cells were described previously (43, 44) and maintained in ascorbic acid-free α-modified Eagle's medium, 10% fetal bovine serum (FBS), and 1% penicillin/streptomycin and were not used beyond passage 15. C2C12 myoblasts, a gift from Dr. Daniel Goldman (University of Michigan, Ann Arbor, MI), C3H10T1/2 fibroblasts (American Type Culture Collection), and 3T3-L1 mouse preadipocytes (American Type Culture Collection) were maintained in Dulbecco's modified Eagle's medium, 10% FBS. F9 teratocarcinoma cells (American Type Culture Collection) and rat ROS17/2.8 osteosarcoma cells (gift from Dr. Laurie McCauley, University of Michigan School of Dentistry) were grown in modified Eagle's medium, 10% FBS.

Yeast Two-hybrid Analysis—A yeast pLexA two-hybrid system (Clontech) was used to identify proteins that bind to mouse Runx2. A cDNA fragment encoding the aa-263–351 region of Runx2 was subcloned into the BamHI/XhoI sites of pLexA, creating an in-frame fusion with the DNA binding domain of the *LexA* gene that is controlled by the strong yeast *ADH1* promoter. The resultant plasmid pLexA-Runx2 (aa 263–351) was then transformed into a yeast reporter strain (YM4271), and the transformed cells (1×10^9) were mated for 24 h with cells (2.5×10^8) of a pretransformed two-hybrid library made from human brain cDNA. The resultant mating mixture was spread on 20 × 10-cm plates to select for expression of the *LEU2* and *lacZ* reporter genes. Approximately 2×10^6 colonies were screened. Sixty four positive colonies were isolated. The prey plasmids were extracted from the positive colonies and the cDNA inserts in the plasmids were amplified by PCR and sequenced. Of the 64 positive colonies, 5 are the full-length *TFIIA*γ cDNAs, and the rest contained 16 different cDNAs.

DNA Constructs and Transfection—p657mOG2-luc, p657mOG2OSE1mt-luc, p657mOG2OSE2mt-luc, p657mOG2-(OSE1 + 2)mt-luc, p4OSE1-luc, p4OSE1mt-luc, p6OSE2-luc, p6OSE2mt-luc, pCMV/β-galactosidase, pCMV/ATF4, pCMV/Runx2, pCMV/FLAG-Runx2 and its deletion mutants (aa 1–330, aa 1–286, and aa-258), GST-Runx2 and GST-ATF4 fusion protein expression vectors were described previously (1, 13, 23, 25, 45). The full-length cDNA of human *TFIIA*-γ was cloned by an RT-PCR strategy using total RNA from human Saos2 osteoblastic cells as a template and specific primers (forward, 5′-ATG GCA TAT CAG TTA TAC AGA AA-3′, and reverse, 5′-TTC TGT AGT ATT GGA GCC AGT A-3′). Digested PCR products were purified and subcloned into the NotI/BamHI sites of the pFLAG-5a expression vector (Sigma). Addition of a C-terminal FLAG sequence into the *TFIIA*-γ cDNA facilitates monitoring of expression levels and immunoprecipitation using M2 antibody (Sigma). GST-TFIIAγ fusion protein expression plasmid was constructed by subcloning the full-length *TFIIA*γ cDNA into the glutathione *S*-transferase gene fusion vector pGEX-4T-1 (Amersham Biosciences) in correct reading frame. The accuracy of DNA sequences was verified by automatic sequencing. The size of expressed proteins was confirmed by Western blot analysis using specific antibodies. For expression and functional studies, cells were plated on 35-mm dishes at a density of 5×10^4 cells/cm^2. After 24 h, cells were transfected with the indicated plasmid DNAs (0.01 μg of pRL-SV40, 0.25 μg of test luciferase reporter, and 1.0 μg of expression plasmids balanced as necessary with β-galactosidase expression plasmid such that the total DNA was constant)

Downloaded from www.jbc.org at University of Pittsburgh on July 4, 2008

and Lipofectamine 2000 (Invitrogen) according to manufacturer's instructions. After 36 h, whole cell extracts were prepared and used for Western blot analysis or dual luciferase assay using the dual luciferase assay kit (Promega, Madison, WI) on a Veritas™ microplate luminometer (Turner Biosystem, Inc., Sunnyvale, CA). Firefly luciferase activity was normalized to *Renilla* luciferase activity for transfection efficiency.

RNA Isolation and Reverse Transcription (RT)—Total RNA was isolated using TRIzol reagent (Invitrogen) according to the manufacturer's protocol. RT was performed using 2 μg of denatured RNA and 100 pmol of random hexamers (Applied Biosystem, Foster, CA) in a total volume of 25 μl containing 12.5 units of MultiScribe reverse transcriptase (Applied Biosystem, Foster, CA) according to the manufacturer's instructions.

Regular PCR—Regular PCR was performed on a 2720 Thermal Cycler (Applied Biosystem, Foster, CA), using 2.5 μl of the cDNA (equivalent to 0.2 μg of RNA) and AmpliTaq DNA polymerase (Applied Biosystems, Foster City, CA) in a 25-μl reaction according to the manufacturer's instructions. The DNA sequences of primers used for PCR were as follows: mouse/rat *TFIIAγ*, 5′-ATG GCA TAT CAG TTA TAC AGA AAT ACA-3′ (forward), 5′-GGT ATT TTT ACC ATC ACA GGC T-3′(reverse); mouse/rat *Atf4*, 5′-ATG GCT TGG CCA GTG CCT CAG A-3′ (forward), 5′-GCT CTG GAG TGG AAG ACA GAA C-3′ (reverse); mouse/rat *Hprt*, 5′-GTT GAG AGA TCA TCT CCA CC-3′ (forward), 5′-AGC GAT GAT GAA CCA GGT TA-3′ (reverse). For all primers the amplification was performed as follows: initial denaturation at 95 °C for 30s followed by 31 cycles of 95 °C for 15 s, 60 °C for 30 s, 72 °C for 30 s and extension at 72 °C for 7 min. The amplified PCR products were run on a 1.2% agarose gel and visualized by ethidium bromide staining.

Quantitative Real Time PCR—Quantitative real time PCR was performed on an iCycler (Bio-Rad) using a SYBR® Green PCR core kit (Applied Biosystem, Foster, CA) and cDNA equivalent to 10 ng of RNA in a 50-μl reaction according to the manufacturer's instructions. The DNA sequences of primers used for real time PCR were as follows: mouse *Ocn*, 5′-TAG TGA ACA GAC TCC GGC GCT A-3′ (forward), 5′-TGT AGG CGG TCT TCA AGC CAT-3′ (reverse); mouse and rat *18 S rRNA*, 5′-CGT CTG CCC TAT CAA CTT TCG ATG GTA G-3′ (forward), 5′-GCC TGC TGC CTT CCT TGG ATG T-3′ (reverse); mouse and rat *TFIIAγ*, 5′-TGG GGA ACA GTC TTC AAG AGA GCC TT-3′ (forward); 5′-TTC CTG ACT CTC TGA GCC AAT GCT G-3′ (reverse); rat *Ocn*, 5′-TGG TGA ATA GAC TCC GGC GCT ACC T-3′ (forward), 5′-CCT GGA AGC CAA TGT GGT CCG-3′ (reverse); rat *Bsp*: 5′-GGC TGG AGA TGC AGA GGG CAA GGC-3′ (forward), 5′-TGG TGC TGG TGC CGT TGA CGA CCT-3′ (reverse); rat *Opn*, 5′-TGG TGA ATA GAC TCC GGC GCT ACC T-3′ (forward), 5′-CCT GGA AGC CAA TGT GGT CCG-3′ (reverse). For all primers the amplification was performed as follows: initial denaturation at 95 °C for 10 min followed by 40 cycles of 95 °C for 15 s and 60 °C for 60 s. Melting curve analysis was used to confirm the specificity of the PCR products. Six samples were run for each primer set. The levels of mRNA were calculated by the Δ*CT* method (46). *Ocn*, *Bsp*, *TFIIAγ*, *osteopontin* (*Opn*), and *Atf4* mRNAs were normalized to *18 S rRNA* mRNA.

Western Blot Analysis—Cells were washed with cold 1× phosphate-buffered saline and lysed in 1× Passive Buffer (Promega, Madison, WI) at room temperature for 20 min. Lysates were clarified by centrifugation (20 min, 13,000 × *g*, 4 °C). Protein concentrations were determined by the method developed by Bio-Rad. Twenty μg of total protein were fractionated on a 10% SDS-polyacrylamide gel and transferred onto nitrocellulose membranes (Schleicher & Schuell). The membrane was blocked in 5% nonfat milk in Tris-buffered saline/Tween 20 (TBST) buffer, probed with antibodies against TFIIA-γ (1:200), TFIIA-α (1:1000), ATF4 (1:1000), Runx2 (1:1000), Fra-1 (1:1000), GST (1:5000), or M2 (1:2000) followed by incubation with anti-goat-mouse or -rabbit antibodies conjugated with horseradish peroxidase (1:5000) and visualized using an enhanced chemiluminescence kit (Pierce). Finally, blots were stripped two times in buffer containing 65 mM Tris-Cl, pH 6.8, 2% SDS, and 0.7% (v/v) β-mercaptoethanol at 65 °C for 15 min and re-probed with β-actin antibody (1:5000) for normalization.

Immunoprecipitation—GST, GST-TFIIAγ, GST-ATF4, and GST-Runx2 fusion proteins were purified using the Bulk GST purification module kit (Amersham Biosciences) according the manufacturer's instructions. Whole cell extracts (500 μg), nuclear extracts (200 μg), or GST fusion proteins (1.0 μg) were pre-cleaned twice with 50 μl of protein A/G-agarose beads (Stratagene, La Jolla, CA) for 30 min followed by pelleting of beads. The protein A/G-agarose beads were blocked with 10 μg/ml bovine serum albumin in 1× phosphate-buffered saline for 1 h before use to reduce nonspecific binding of proteins. Five μg of respective antibody was added and incubated for 2 h at 4 °C with gentle rocking. The immune complexes were collected by addition of 30 μl of protein A/G-agarose beads and incubation for 1 h at 4 °C followed by centrifugation. Precipitates were washed five times with 1× washing buffer (20 mM HEPES, pH 7.6, 50 mM KCl, 1 mM dithiothreitol, 0.25% Nonidet P-40, 5 mM NaF, 1 mM EGTA, 5 mM $MgCl_2$, 0.25 mM phenylmethylsulfonyl fluoride), and the immunoprecipitated complexes were suspended in SDS sample buffer and analyzed by SDS-PAGE followed by Western blot analysis using the indicated antibodies.

ChIP Assays—ChIP assays were performed as described previously (41) using a protocol kindly provided by Dr. Dwight Towler (Washington University) (47). After sonication, the amount of chromatin was quantified using the PicoGreen double-stranded DNA quantitation assay (Molecular Probes) according to the manufacturer's instructions. The equivalent of 10 μg of DNA was used as starting material (input) in each ChIP reaction with 2 μg of the appropriate antibody (TFIIAγ, or control rabbit IgG). Fractions of the purified ChIP DNA (5%) or inputs (0.02–0.05%) were used for PCR analysis. The reaction was performed with AmpliTaq Gold DNA polymerase (Applied Biosystems) for 35 cycles of 60 s at 95 °C, 90 s at 58 °C, and 120 s at 68 °C. PCR primer pairs were generated to detect DNA segments located near the Runx2-binding site at −137/−131 (primers P1 and P2), ATF4-binding site at −55/−48 (primers P3 and P4) in mouse *osteocalcin* gene 2 (*mOG2*) proximal promoter, or the Runx2-binding site located between −370 and −42 in the proximal mouse *Runx2* promoter region (primers

Downloaded from www.jbc.org at University of Pittsburgh on July 4, 2008

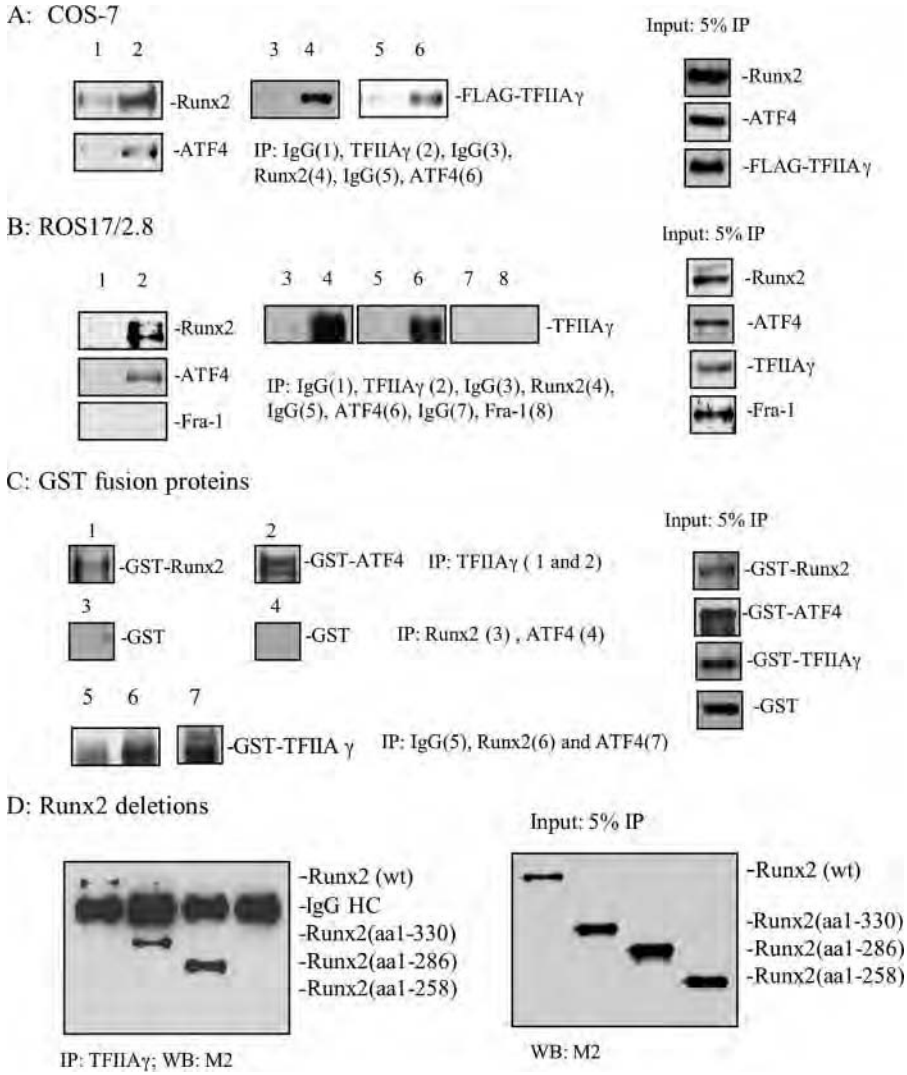

FIGURE 1. **Protein-protein interactions among TFIIAγ, Runx2, and ATF4.** *A,* whole cell extracts from COS-7 cells overexpressing pFLAG-TFIIAγ, pCMV-Runx2, and pCMV-ATF4 were immunoprecipitated (*IP*) with normal IgG (*lane 1*) or TFIIAγ antibody (*lane 2*) followed by Western blot (*WB*) analysis using Runx2 or ATF4 antibodies. In reciprocal IPs, the same extracts were immunoprecipitated with normal IgG (*lanes 3* and *5*), Runx2 antibody (*lane 4*), or ATF4 antibody (*lane 6*) followed by WB using M2 antibody. *B,* nuclear extracts from ROS17/2.8 cells were immunoprecipitated with normal IgG (*lane 1*) or TFIIAγ antibody (*lane 2*) followed by WB using Runx2, ATF4, or Fra-1 antibodies. In reciprocal IPs, the same extracts were immunoprecipitated with normal IgG (*lanes 3, 5* and *7*), Runx2 antibody (*lane 4*), ATF4 antibody (*lane 6*), or Fra-1 antibody (*lane 8*) followed by WB using TFIIAγ antibody. *C,* mixture of purified GST-TFIIAγ and GST-Runx2 was immunoprecipitated by TFIIAγ antibody followed by WB for Runx2 (*lane 1*). A mixture of purified GST-TFIIAγ and GST-ATF4 was immunoprecipitated by TFIIAγ antibody followed by WB for ATF4 (*lane 2*). A mixture of purified GST and GST-Runx2 was immunoprecipitated by Runx2 antibody followed by WB for GST (*lane 3*). A mixture of purified GST and GST-ATF4 was immunoprecipitated by ATF4 antibody followed by WB for GST (*lane 4*). In reciprocal IPs, a mixture of purified GST-TFIIAγ and GST-Runx2 was immunoprecipitated by normal IgG (*lane 5*) or Runx2 antibody (*lane 6*) followed by WB for TFIIAγ. A mixture of purified GST-TFIIAγ and GST-ATF4 was immunoprecipitated by ATF4 antibody (*lane 7*) followed by WB for TFIIAγ. *D,* nuclear extracts from ROS17/2.8 cells were mixed with equal amount of nuclear extracts from COS-7 cells overexpressing FLAG-Runx2(wt), FLAG-Runx2 (aa 1–330), FLAG-Runx2 (aa 1–286), and FLAG-Runx2 (aa 1–258), and immunoprecipitated with TFIIAγ antibody followed by WB for Runx2 (M2 antibody). Experiments were repeated 2–3 times, and qualitatively identical results were obtained.

P5 and P6) (48), and the *mOG2* gene region (+177/+311) (primers P7 and P8) (see Fig. 2*A* and Table 1). The PCR products were separated on 3% agarose gels and visualized with ultraviolet light. All ChIP assays were repeated at least three times.

siRNA—ROS17/2.8 osteoblast-like cells, which contain high levels of TFIIAγ protein, were transfected with mouse *TFIIAγ* siRNA kit (Santa Cruz Biotechnology) or negative control siRNA(low GC, catalog number 12935-200, Invitrogen) using Lipofectamine 2000 (Invitrogen) according the manufacturer's instruction. After 36 h, total RNA was harvested for quantitative real time RT-PCR analysis for *TFIIAγ*, *Ocn, Bsp, Opn* (*osteopontin*), and *Atf4* mRNAs. A second set of mouse *TFIIAγ* siRNAs (sense, AUG ACA ACA CUG UGC UAU AUU; antisense, UAU AGC ACA GUG UUG UCA UUU) was designed in the project laboratory and used to confirm the results using the first set of *TFIIAγ* siRNA.

Statistical Analysis—Results were expressed as means ± S.D. Students' *t* test was used to test for differences between two groups. Differences with a $p < 0.05$ was considered as statistically significant.

RESULTS

TFIIAγ Interacts with Runx2 and ATF4—A yeast pLexA two-hybrid system (Clontech) was used to identify proteins that bind to mouse Runx2. cDNA fragments encoding several C-terminal regions of Runx2 were subcloned into the BamHI/XhoI sites of pLexA, creating in-frame fusions with the DNA binding domain of the *LexA* gene that is controlled by the strong yeast *ADH1* promoter. Preliminary experiments using relatively larger regions of Runx2 (aa 232–391, aa 232–428, and aa 232–517) as baits were not successful because of their ability to autoactivate the *lacZ* reporter gene in yeast. In contrast, by using the aa 263–351 region of Runx2 as a bait, we identified TFIIAγ, a general transcriptional factor involved in the initiation step of eukaryotic transcription, as a Runx2-interacting factor. A diagram and a picture of a positive colony are shown in Fig. S1.

To verify the TFIIAγ-Runx2 interaction identified by yeast two-hybrid system, we conducted pulldown assays. COS-7 cells were transiently transfected with expression vectors for FLAG-TFIIAγ, Runx2, and ATF4 (a recently identified Runx2-interacting factor). After 36 h, whole cell extracts were prepared for immunoprecipitation (IP) assay using a TFIIAγ antibody followed by Western blot analysis for Runx2 and ATF4. As seen in Fig. 1*A* (*lane 2*), Runx2 protein was present in a TFIIAγ anti-

Downloaded from www.jbc.org at University of Pittsburgh on July 4, 2008

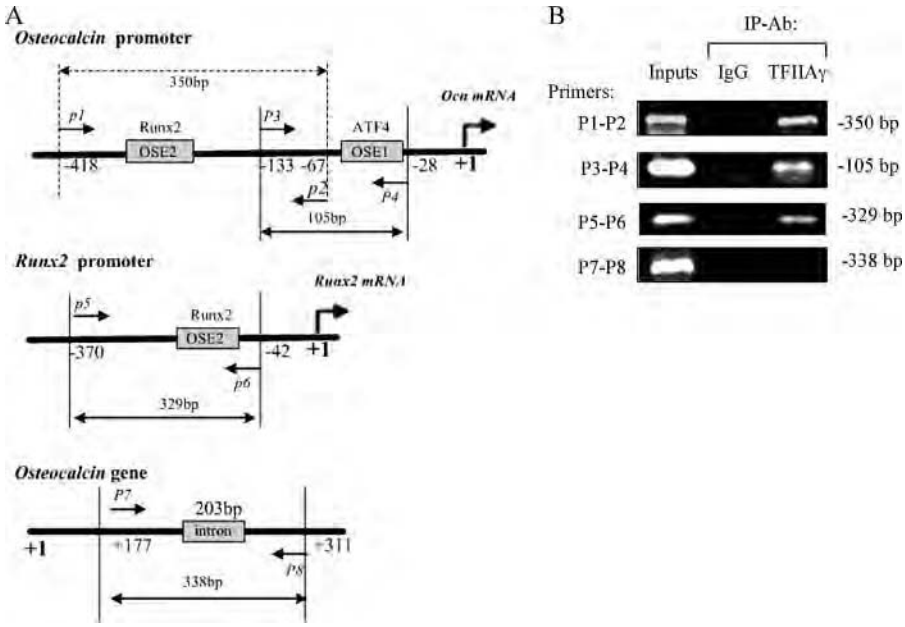

FIGURE 2. **ChIP analysis of TFIIAγ interaction with Runx2/ATF4 binding sites-containing chromatin fragments of *mOG2* promoter in MC-4 cells.** *A,* schematic representation of relevant regions of the *mOG2* promoter, mouse *Runx2* promoter, and *mOG2* gene. P1, P2, P3, P4, P5, P6, P7, and P8 indicate PCR primers used to analyze ChIP DNAs. The positions of these primers and the size of the fragments they amplify are indicated at the top or bottom of the figure. *B,* MC-4 cells were seeded at a density of 50,000 cells/cm^2 in 35-mm dishes, cultured in 10% FBS medium overnight, and cross-linked with formaldehyde for ChIP assays. IPs were conducted with TFIIAγ antibody (*Ab*) or normal control IgG. PCR products were run on 3% agarose gel and stained with ethidium bromide. Purified input chromatin was used to perform parallel PCRs with the respective primer pairs. Experiments were repeated three times with similar results.

TABLE 1
PCR primers used in ChIP assay

Oligonucleotide name	Sequence
P1	CCGCTCTCAGGGGCAGAC
P2	AGGGGATGCTGCCAGGACTAAT
P3	CACAGCATCCTTTGGGTTTGAC
P4	TATCGGCTACTCTGTGCTCTCTGA
P5	GCTATA ACCTTCTT AATGCCAG
P6	AGCACTATTACTGGAGAGACAGAATC
P7	TAGTGAACAGACTCCGGCGCTA
P8	TGTAGGCGGTCTTCA AGCCAT

body immunoprecipitate. Interestingly, anti-TFIIAγ antibody also immunoprecipitated ATF4. Reciprocal IPs showed that both Runx2 and ATF4 antibodies immunoprecipitated the FLAG-tagged TFIIAγ (Fig. 1*A*, *lanes 4* and *6*). To determine whether TFIIAγ can interact with Runx2 and ATF4 in osteoblasts, nuclear extracts from ROS17/2.8 cells that express high levels of Runx2, ATF4, and TFIIAγ were immunoprecipitated with anti-TFIIAγ antibody followed by Western blot analysis for Runx2, ATF4, or Fra-1 (a member of AP1 family). Results show that both Runx2 and ATF4 but not Fra-1 proteins were present in anti-TFIIAγ immunoprecipitates (Fig. 1*B*, *lane 2*). Reciprocal IPs showed that antibodies against Runx2 or ATF4 but not Fra-1 immunoprecipitated TFIIAγ in ROS17/2.8 cells (Fig. 1*B*, *lanes 4, 6,* and *8*). Normal control IgG failed to significantly pull down Runx2, ATF4, or TFIIAγ in either COS-7 cells or osteoblasts. Taken together, these studies confirm that TFIIAγ interacts with Runx2 and ATF4 in osteoblasts or when coexpressed in COS-7 cells.

Although Runx2 and ATF4 interact in osteoblasts, IP assays using purified GST fusion proteins failed to show a direct physical interaction between ATF4 and Runx2 (25), suggesting that accessory factors may be involved in their interactions. To determine whether TFIIAγ can directly interact with Runx2 or ATF4 in the absence of other nuclear proteins, we mixed GST or GST-TFIIAγ with GST-ATF4 or GST-Runx2 fusion proteins purified from *Escherichia coli*, followed by IP and Western blot analysis. As shown in Fig. 1*C*, both GST-Runx2 and GST-ATF4 proteins mixed with GST-TFIIAγ were immunoprecipitated by anti-TFIIAγ antibody (*lanes 1* and *2*). Anti-Runx2 or anti-ATF4 antibody was unable to immunoprecipitate GST protein mixed with GST-Runx2 (Fig. 1*C*, *lane 3*) or GST-ATF4 (*lane 4*). Reciprocal IPs show that GST-TFIIAγ was immunoprecipitated by both anti-Runx2 or anti-ATF4 antibodies (Fig. 1*C*, *lanes 6* and *7*) but not by normal control IgG (*lane 5*). These results demonstrate that TFIIAγ directly binds to both Runx2 and ATF4.

As a first step to identify the TFIIAγ-binding domain, FLAG-Runx2 deletion mutant expression vectors (wild type aa 1–528, aa 1–330, aa 1–286, and aa 1–258) were transfected into COS-7 cells because of the high transfection efficiency. Nuclear extracts were prepared 36 h later, mixed with equal amounts of nuclear extracts of ROS17/2.8 (which contain large amounts of endogenous TFIIAγ), and immunoprecipitated using anti-TFIIAγ antibody followed by Western blot analysis for Runx2 (M2 antibody). As shown in Fig. 1*D*, deletion of Runx2 from aa 528 to aa 286 did not reduce TFIIAγ binding. However, further deletion from aa 286 to aa 258 completely abrogated TFIIAγ-Runx2 complex formation. These data clearly demonstrate the following: (i) endogenous TFIIAγ can interact with overexpressed FLAG-Runx2 proteins *in vitro*; and (ii) the aa 258–286 region of Runx2 is required for TFIIAγ binding. Interestingly, this same region is required for ATF4-Runx2 interactions (25).

To determine whether, in intact cells, TFIIAγ is associated with the endogenous *osteocalcin* gene 2 (*mOG2*) promoter region that has been shown to bind Runx2 and ATF4, we performed the chromatin immunoprecipitation (ChIP) assay using MC3T3-E1 (clone MC-4) preosteoblast cells. After shearing, soluble chromatin was immunoprecipitated with either an antibody against TFIIAγ or control IgG. The positions and sequences of primers used for PCR analysis of ChIP DNAs are shown in Fig. 2*A* and Table 1. As shown in Fig. 2*B*, the PCR bands amplified with primers P1/P2 and P3/P4 and corresponding to ChIP DNAs immunoprecipitated with TFIIAγ antibody revealed that TFIIAγ specifically interacts with chromatin fragments of the proximal *mOG2* promoter that contain Runx2- or ATF4-binding sites. Furthermore, TFIIAγ antibody

Downloaded from www.jbc.org at University of Pittsburgh on July 4, 2008

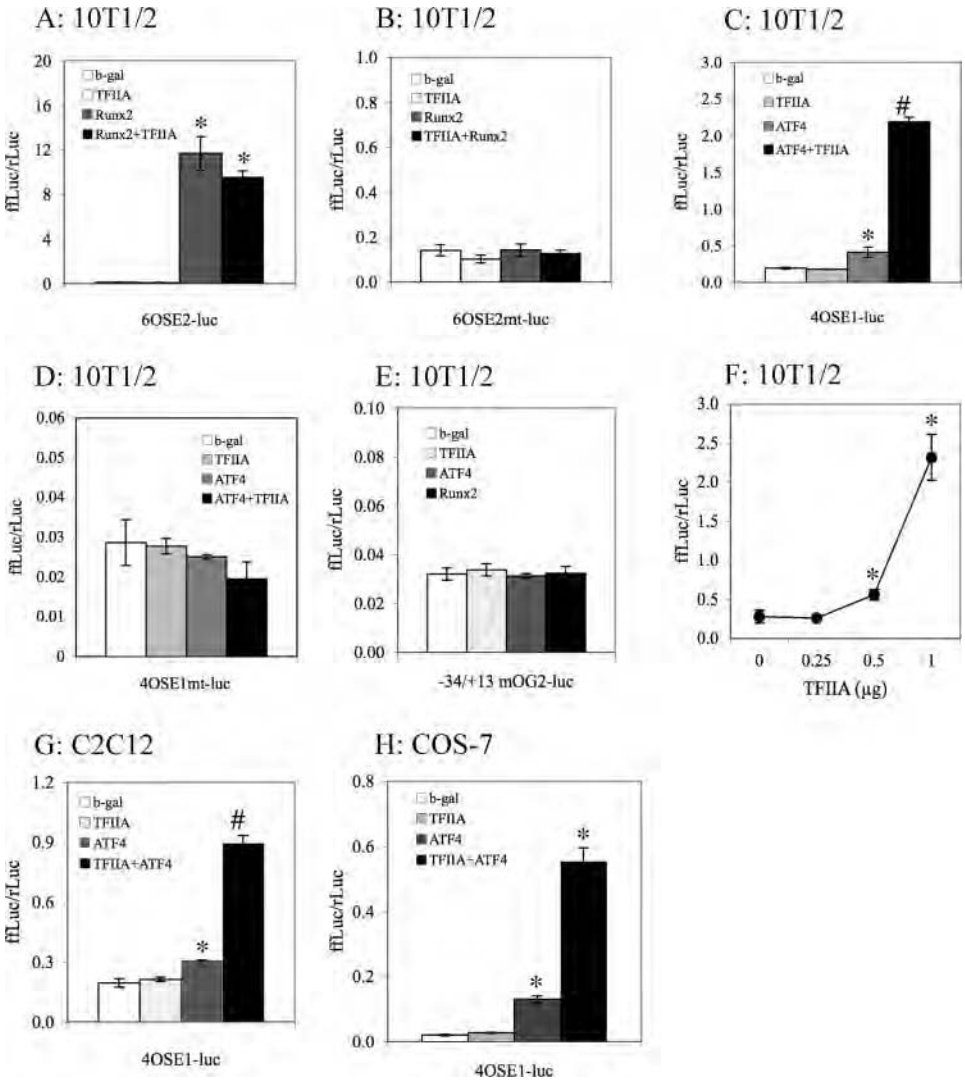

FIGURE 3. **TFIIAγ increases ATF4 but not Runx2 transcriptional activity.** *A* and *B*, 10T1/2 cells were transiently transfected with p6OSE2-luc (*A*) or p6OSE2mt-luc (*B*) and pRL-SV40 (for normalization) and expression plasmids for β-galactosidase, TFIIAγ, Runx2, or Runx2 plus TFIIAγ. After 36 h, cells were harvested for dual luciferase assay. Firefly luciferase was normalized to *Rotylenchulus reniformis* luciferase to control the transfection efficiency (*, $p < 0.01$(β-galactosidase *versus* Runx2 or Runx2+TFIIAγ). *C* and *D*, 10T1/2 cells were transiently transfected with p4OSE2-luc (*C*) or p4OSE1mt-luc (*D*) and pRL-SV40 and expression plasmids for β-galactosidase, TFIIAγ, ATF4, or ATF4 plus TFIIAγ. *, $p < 0.01$ (β-galactosidase *versus* ATF4 or ATF4+TFIIAγ); #, $p < 0.01$(ATF4 *versus* ATF4+TFIIAγ). *E*, 10T1/2 cells were transiently transfected with −34/+13 mOG2-luc and pRL-SV40 and expression plasmids for β-galactosidase, TFIIAγ, ATF4, or Runx2. *F*, dose-response experiment, 10T1/2 cells were transiently transfected with p4OSE1-luc and pRL-SV40 and ATF4 expression plasmid and increasing amounts of TFIIAγ plasmid. *, $p < 0.01$ (β-galactosidase *versus* TFIIAγ). *G* and *H*, C2C12 (*G*) and COS-7 cells (*H*) were transiently transfected with p4OSE2-luc and pRL-SV40 and expression plasmids for β-galactosidase, TFIIAγ, ATF4, or ATF4 plus TFIIAγ. *, $p < 0.01$ (β-galactosidase *versus* ATF4 or ATF4+TFIIAγ). Data represent mean ± S.D. Experiments were repeated three times and qualitatively identical results were obtained. Note the expanded scale for the mutant reporters (*B, D,* and *E*) because of low basal activity to enable visualization of any potential differences as a consequence of cotransfection with the expression vectors noted above.

also immunoprecipitated a Runx2-binding site-containing chromatin fragment of the proximal *Runx2* promoter (primers P5/P6). In contrast, TFIIAγ antibody failed to immunoprecipitate a chromatin fragment of *mOG2* gene that contains no Runx2- or ATF4-binding sites (primers P7/P8). Taken together, these data show that TFIIAγ is recruited to a chromatin fragment of the *mOG2* promoter that was previously demonstrated to be bound by Runx2 and ATF4 in osteoblasts (13, 22).

TFIIAγ Increases ATF4 but Not Runx2-dependent Transcriptional Activity—To determine whether *TFIIAγ* increases Runx2- and ATF4-dependent transcriptional activity, we measured the ability of TFIIAγ to stimulate transcription of p6OSE2-luc, a reporter plasmid containing 6 copies of the Runx2-binding element OSE2 upstream of a minimal 34-bp *mOG2* promoter (13, 43, 49) or p4OSE1-luc, a reporter plasmid that contains four copies of OSE1 (a specific ATF4-binding element) upstream of a minimal 34-bp *mOG2* promoter (22, 25). For these studies, we used C3H10T1/2 fibroblasts because they contain undetectable levels of both endogenous Runx2 and ATF4 proteins (28, 49). As shown in Fig. 3*A*, as expected, Runx2 alone increased OSE2 transcriptional activity by 11-fold. This stimulation was abolished in the 6OSE2mt-luc in which the OSE2 core sequence was mutated (25) (Fig. 3*B*). Although we have shown above that TFIIAγ interacts with Runx2, TFIIAγ transfection did not activate basal or Runx2-dependent OSE2 transcription (Fig. 3*A*). As shown in Fig. 3*C*, ATF4 activated OSE1 activity about 2-fold ($p < 0.01$, β-galactosidase *versus* ATF4). Although TFIIAγ alone was unable to activate OSE1 activity, unexpectedly, when coexpressed with ATF4, it dramatically increased OSE1 activity 5-fold above ATF4 alone. This stimulation was abolished in 4OSE1mt-luc, in which the OSE1 core sequence was mutated from TTACATCA to TTAGTACA in the reporter plasmid (45) (Fig. 3*D*). Note: TFIIAγ, Runx2, or ATF4 failed to activate a minimal 34-bp *mOG2* promoter that contains a TATA box (23, 50) (Fig. 3*E*). Fig. 3*F* shows that TFIIAγ activated ATF4 transcription activity in a dose-dependent manner in C3H10T1/2 cells. TFIIAγ similarly stimulated ATF4-directed OSE1 activity in C2C12 myoblasts (3-fold) and COS-7 cells (4.3-fold) (Fig. 3, *G* and *H*).

TFIIAγ Expression in Different Cell Lines—The levels of *TFIIAγ* mRNAs and proteins were determined in different cell lines by RT-PCR and Western blot analysis, respectively. As shown in Fig. 4, Western blot analysis shows that TFIIAγ protein was expressed at high levels in osteoblastic cells (MC-4

Downloaded from www.jbc.org at University of Pittsburgh on July 4, 2008

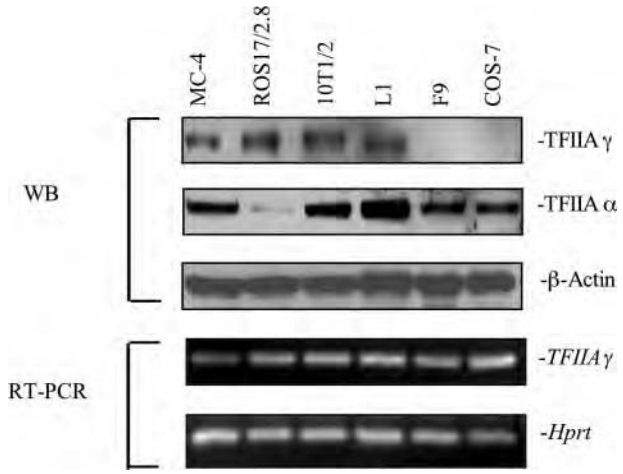

FIGURE 4. **TFIIAγ expression in different cell lines.** Total RNAs or whole cell extracts were prepared from MC-4, ROS17/2.8, 10T1/2, L1, F9, and COS-7 cells and used for RT-PCR and Western blot analysis for levels of TFIIAα and TFIIAγ mRNAs and proteins. Experiments were repeated three times with similar results.

cells and ROS17/2.8), C3H10T1/2 fibroblasts, and L1 preadipocytes. In contrast, levels of TFIIAγ protein were undetectable in F9 teratocarcinoma cells and COS-7 (transformed African green monkey kidney fibroblasts). Interestingly, *TFIIAγ* mRNA was ubiquitously expressed in these cell lines. In addition, TFIIAα proteins were present in all these cell lines except for ROS17/2.8 cells, which contain a low level of TFIIAα protein.

TFIIAγ Stimulation of Endogenous Ocn mRNA Expression and the 657-bp mOG2 Promoter Activity Is Dependent upon the Presence of ATF4 and Runx2—ATF4 is an osteoblast-enriched protein that is required for late osteoblast differentiation (*i.e. Ocn* and *Bsp* mRNA expression) and bone formation *in vivo*. Our recent study demonstrated that ATF4 activation of *mOG2* promoter activity and *Ocn* mRNA expression was dependent upon the presence of Runx2 via a mechanism involving protein-protein interactions (25). To determine the effects of TFIIAγ on endogenous *Ocn* mRNA expression, C3H10T1/2 cells were transiently transfected with expression vectors for β-galactosidase, TFIIAγ, ATF4, Runx2, ATF4/Runx2, TFIIAγ/Runx2, TFIIAγ/ATF4, and ATF4/Runx2/TFIIAγ. After 36 h, cells were harvested for RNA preparation and quantitative real time RT-PCR detection of *Ocn* mRNA. As shown in Fig. 5*A*, consistent with its role as a master gene of osteoblast differentiation, Runx2 alone increased endogenous *Ocn* expression by 3.3-fold ($p < 0.01$; β-galactosidase *versus* Runx2). TFIIAγ alone, ATF4 alone, and TFIIAγ/ATF4 were all not sufficient for activation of endogenous *Ocn* mRNA expression. TFIIAγ alone did not enhance Runx2-dependent *Ocn* expression. As demonstrated previously (25), ATF4 dramatically stimulated Runx2-dependent *Ocn* mRNA expression by 10-fold ($p < 0.01$, Runx2 *versus* Runx2/ATF4). Importantly, TFIIAγ further augmented *Ocn* mRNA expression 4.2-fold in the presence of ATF4 and Runx2 ($p < 0.01$, ATF4/Runx2 *versus* ATF4/Runx2/TFIIAγ). TFIIAγ similarly enhanced ATF4/Runx2-dependent 657-bp *mOG2* promoter activity in C3H0T1/2 cells (3.6-fold) (Fig. 5*B*) ($p < 0.01$, ATF4/Runx2 *versus* ATF4/Runx2/TFIIAγ). This stimulation was completely abolished by point mutations in the OSE1 and/or OSE2 core sequences.

Silencing of TFIIAγ Markedly Reduces Levels of Endogenous Ocn and Bsp mRNAs and ATF4 Protein in Osteoblasts—To determine whether TFIIAγ is required for the endogenous *Ocn* mRNA expression in osteoblasts, we knocked down the endogenous *TFIIAγ* transcripts by siRNA. ROS17/2.8 osteoblast-like cells, which express high levels of *TFIIAγ* and *Ocn* and *Bsp* mRNAs, were transiently transfected with *TFIIAγ* siRNA reagent from Santa Cruz Biotechnology according to the manufacturer's instructions. This siRNA is a pool of three specific 20–25-nucleotide siRNA targeting both mouse and rat *TFIIAγ*. As shown in Fig. 6*A*, quantitative real time RT-PCR analysis showed that levels of *TFIIAγ* mRNA were efficiently reduced by *TFIIAγ* siRNA in a dose-dependent manner. The level of *Ocn* mRNA was reduced greater than 50% by *TFIIAγ* siRNA ($p < 0.01$, control *versus TFIIAγ* siRNA). Interestingly, *Bsp* mRNA, another ATF4 downstream target gene (22), was also reduced by 50% ($p < 0.01$, control *versus TFIIAγ* siRNA). This inhibition was specific because levels of *Opn* and *Atf4* mRNAs were not reduced by *TFIIAγ* siRNA. In contrast, as shown in Fig. 6*B*, levels of all these mRNAs were not reduced by the negative control siRNA (Invitrogen). Although *Atf4* mRNA was not altered by *TFIIAγ* siRNA, the level of endogenous ATF4 protein was significantly reduced by silencing *TFIIAγ* in osteoblasts (Fig. 6*C*). Similar results were obtained when a different set of TFIIAγ siRNA was used (Fig. S2).

Overexpression of TFIIAγ Increases the Levels of ATF4 Protein—The above studies clearly demonstrated that TFIIAγ increased ATF4-dependent transcription activity and *Ocn* gene expression probably by targeting ATF4 protein. To further study the mechanism of this regulation, we determined the effect of TFIIAγ overexpression on the levels of ATF4 protein. C3H10T1/2 cells, which express undetectable level of endogenous ATF4 protein (28), were transiently transfected with 1.0 μg of ATF4 expression plasmid and increasing amounts of TFIIAγ expression plasmid (0, 0.5, 1, and 2 μg). After 36 h, cells were harvested for Western blot analysis. As shown in Fig. 7*A*, overexpression of TFIIAγ in C3H10T1/2 cells increased the levels of ATF4 protein in a dose-dependent manner. This increase in ATF4 protein was specific because levels of Runx2 were not altered by TFIIAγ. TFIIAγ similarly elevated levels of ATF4 protein in COS-7 cells (Fig. 7*B*). Next, we determined if TFIIAγ could increase the levels of endogenous ATF4 proteins in osteoblasts. ROS17/2.8 cells were transiently transfected with indicated amount of TFIIAγ expression vector. Western blot analysis shows that TFIIAγ dose-dependently increased levels of endogenous ATF4 protein in ROS17/2.8 cells (Fig. 7*C*). Similar results were obtained in MC-4 cells (Fig. 7*D*). Interestingly, overexpression of TFIIAγ did not increase the levels of *Atf4* mRNA in all these cells examined (*bottom*, Fig. 7, *A–D*). Taken collectively, TFIIAγ markedly increased levels of ATF4 proteins in osteoblasts and non-osteoblasts.

TFIIAγ Increases ATF4 Protein Stability—Lassot *et al.* (51) recently showed that acetylase p300 markedly increased the levels of ATF4 protein and ATF4-dependent transcriptional activity by inhibiting ATF4 protein degradation via a proteasomal ubiquitin pathway. As an initial step to determine whether TFIIAγ alters ATF4 protein stability, C3H10T1/2 cells were

Downloaded from www.jbc.org at University of Pittsburgh on July 4, 2008

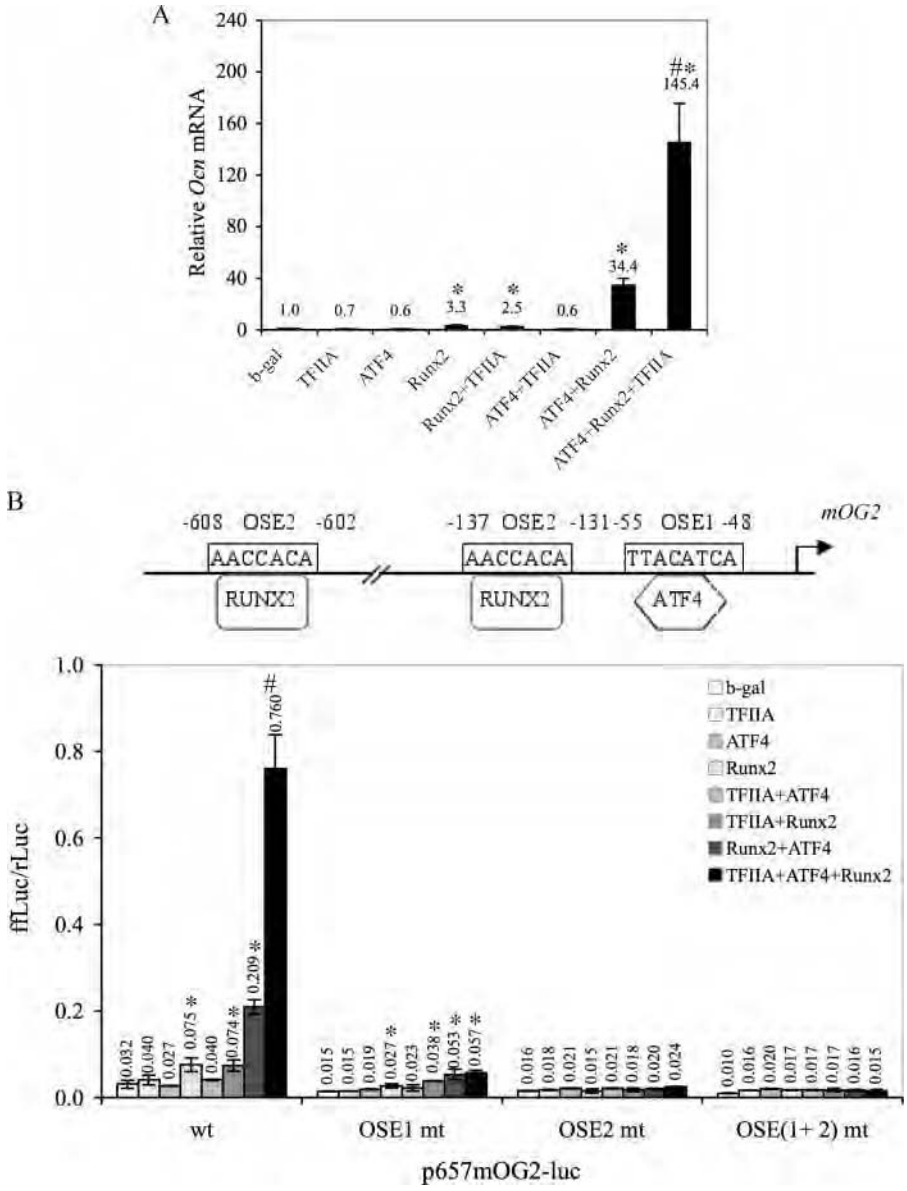

FIGURE 5. **TFIIAγ activates endogenous *Ocn* gene expression and 0.657-kb *mOG2* promoter activity in the presence of ATF4 and Runx2.** *A,* 10T1/2 cells were transfected with expression plasmids for β-galactosidase (*β-gal*), TFIIAγ, ATF4, Runx2, Runx2/TFIIAγ, ATF4/TFIIAγ, ATF4/Runx2, or ATF4/TFIIAγ/Runx2. After 36 h, the cells were harvested for RNA isolation and quantitative real time RT/PCR analysis for *Ocn* mRNA. *B,* 10T1/2 cells were transfected with p657mOG2-luc or p657mOG2OSE1mt-luc or p657mOG2OSE2mt-luc or p657mOG2OSE(1 + 2)mt-luc, pRL-SV40, and expression plasmids for β-galactosidase, TFIIAγ, ATF4, Runx2, Runx2/TFIIAγ, ATF4/TFIIAγ, ATF4/Runx2, or ATF4/TFIIAγ/Runx2. After 36 h, the cells were harvested for dual luciferase assay. *, $p < 0.01$ (β-galactosidase *versus* Runx2, or ATF4+Runx2 or ATF4+Runx2+TFIIAγ); #, $p < 0.01$(ATF4+Runx2 *versus* ATF4+Runx2+TFIIAγ). Data represent mean ± S.D. Experiments were repeated 3–4 times and qualitatively identical results were obtained.

transiently transfected with ATF4 expression vector in the presence of β-galactosidase, TFIIAγ, or Runx2 expression vectors. After 36 h, cells were treated with 50 μg/ml of protein synthesis inhibitor cycloheximide (CHX) (*i.e.* to completely block *de novo* protein synthesis) and harvested at different time points of CHX addition (0, 0.5, 1, and 3 h) followed by Western blot analysis for ATF4 and Runx2. This technique has been widely used to study protein stability (51). As shown in Fig. 8*A*, in the absence of TFIIAγ overexpression, ATF4 protein was rapidly degraded and almost undetectable on Western blot by 3 h after CHX addition, which is consistent with a previous study (51). However, overexpression of TFIIAγ greatly delayed the degradation process with the levels of ATF4 protein only slightly reduced by 3 h after CHX addition. In contrast, levels of Runx2 protein were not affected by TFIIAγ (Fig. 8*B*).

DISCUSSION

This study identifies TFIIAγ as a bridging molecule between Runx2, ATF4, and the transcription machinery in osteoblasts. Although Runx2 and ATF4 interact in osteoblasts or when coexpressed in COS-7 cells, IPs using purified GST fusion proteins were unable to demonstrate a direct physical interaction between ATF4 and Runx2 (25). Thus, accessory factors are likely involved in bridging these two molecules. Several lines of evidence support that TFIIAγ may be a factor linking Runx2 and ATF4. (i) TFIIAγ forms complexes with both Runx2 and ATF4 in osteoblasts and when coexpressed in COS-7 cells. (ii) The same region of Runx2 (*i.e.* aa 258–286) is required for both TFIIAγ-Runx2 and ATF4-Runx2 interactions. (iii) Purified GST-TFIIAγ fusion protein directly binds to both purified GST-Runx2 and GST-ATF4 fusion proteins. (iv) Overexpression of TFIIAγ in 10T1/2 cells dramatically enhances endogenous *Ocn* gene expression and the 657-bp *mOG2* promoter activity in the presence of ATF4 and Runx2. (v) siRNA knockdown of *TFIIAγ* mRNA markedly reduces osteoblast-specific *Ocn* and *Bsp* expression.

Accumulating evidence establishes that ubiquitin-proteasome pathways control osteoblast differentiation and bone formation. For example, the proteasome inhibitors epoxomicin and proteasome inhibitor-1, when administered systemically to mice, strongly stimulated bone volume and bone formation rates by greater than 70% after only 5 days of treatment (52). Although the mechanism of this regulation remains unclear, critical bone transcription factors seem to be targets for the ubiquitin-proteasomal pathway. Zhao and co-workers (52, 53) recently showed that Smurf1, an E3 ubiquitin-protein isopeptide ligase, accelerated Runx2 ubiquitin-proteasomal degradation and inhibited osteoblast differentiation and bone forma-

Downloaded from www.jbc.org at University of Pittsburgh on July 4, 2008

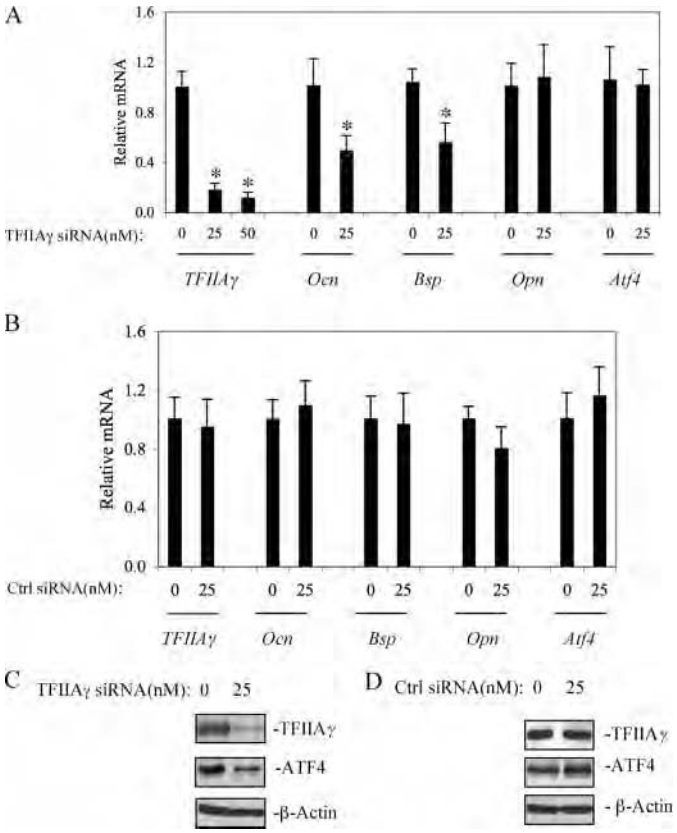

FIGURE 6. **TFIIAγ siRNA blocks endogenous *Ocn* mRNA expression in osteoblastic cells.** ROS17/2.8 osteoblast-like cells were transiently transfected with *TFIIAγ* siRNA (*A*) or negative control (*Ctrl*) siRNAs (*B*). After 36 h, total RNA or whole cell extracts were prepared for quantitative real time RT-PCR analysis for *TFIIAγ*, *Ocn*, *Bsp*, *Opn*, and *Atf4* mRNAs which were normalized to the *18 S rRNA* mRNAs or Western blot analysis for ATF4, TFIIAγ, and β-actin (*C* and *D*). *, $p < 0.01$ (control *versus* siRNA). Data represent mean ± S.D. Experiments were repeated three times with similar results.

tion *in vitro* and *in vivo*. Although *Atf4* mRNA is ubiquitously expressed, in most cells ATF4 proteins are rapidly degraded via the ubiquitin-proteasome pathway with a half-life of 30–60 min. However, this degradation pathway is less active in osteoblasts, thereby allowing ATF4 accumulation (28). Indeed, inhibition of the ubiquitin/proteasomal pathway by MG115, which blocks the N-terminal threonine in the active site of β-subunit of 26 S proteasomal complex (29, 30), led to ATF4 accumulation and induced *Ocn* mRNA expression in non-osteoblastic cells (28). Similarly, silencing of *β-TrCP1*, an E3 ubiquitin-protein isopeptide ligase that interacts with ATF4, by RNA interference, resulted in ATF4 accumulation and increased *Ocn* expression. Thus, ATF4 is a major target of the uquibitin-proteasome pathway, and modulation of ATF4 stability may play a critical role in the regulation of osteoblast-specific gene expression. Because *β-TrCP1* is present in osteoblasts (28), other factor(s) must be present in these cells to protect ATF4 from the proteasomal degradation that occurs in other cell types. Experiments from this study show that overexpression of TFIIAγ dose-dependently increases ATF4 protein in osteoblasts (ROS17/2.8 and MC-4 cells) and non-osteoblasts (C3H10T1/2 and COS-7 cells) without altering *Atf4* mRNA. Experiments using the protein synthesis inhibitor CHX further demonstrate that TFIIAγ greatly inhibits ATF4 degradation. TFIIAγ siRNA decreases ATF4 stability in osteoblasts. Lassot *et al.* (51) recently found that ATF4 is similarly stabilized by cofactor p300, a histone acetyltransferase. p300 inhibits ATF4 ubiquitination and degradation through interaction with the ATF4 N terminus. Interestingly, this stabilization does not require either the acetyltransferase activity of p300 or the serine residue 219 in the context of DSG*XXX*S within ATF4 molecule that is known to be required for ATF4 degradation via the $SCF^{\beta TrCP}$ and the 26 S proteasome (51).

TFIIAγ stimulation of *Ocn* gene transcription is dependent on the presence of both ATF4 and Runx2. As a master regulator of osteoblast differentiation, Runx2 alone is sufficient to activate expression of many osteoblast-specific genes, including *Ocn* and *Bsp*, by direct binding to their promoters (13). In contrast, although ATF4 directly binds to the OSE1 site of the mouse *Ocn* gene and activates OSE1, it alone is not sufficient for activation of the endogenous *Ocn* gene or the 657-bp *mOG2* promoter which contains sufficient information for the bone-specific expression of *Ocn in vivo* (54). Instead, ATF4 stimulation of *Ocn* is dependent on the presence of Runx2 as demonstrated by our recent study (25). ATF4 interacts with Runx2 and activates Runx2-dependent transcriptional activity. A recent study shows that SATB2, a nuclear matrix protein that directly interacts with both ATF4 and Runx2, activates osteoblast differentiation and controls craniofacial patterning *in vivo* (55). This study shows that although TFIIAγ interacts with Runx2, it does not directly activate Runx2. Like ATF4, TFIIAγ alone is not sufficient to activate transcription from either the *Ocn* gene or the 657-bp *mOG2* promoter. In fact, even TFIIAγ and ATF4 together are not sufficient for *Ocn* gene expression without the presence of Runx2 (Fig. 5). However, in the presence of both ATF4 and Runx2, TFIIAγ greatly activates *Ocn* gene expression.

General transcription factors were originally defined as such because they were thought to be universally required for transcription. In eukaryotic cells, initiation of transcription is a complex process, which requires RNA polymerase II and many other basal transcription factors and/or cofactors, including TFIIA, TFIIB, TFIID (TBP or TATA box-binding protein), TFIIE, TFIIF, and TFIIH (56–59). Binding of TBP to the TATA box is the first step, which is regulated by TFIIA. TFIIA enhances transcription by interacting with TBP and stabilizing its binding to DNA (32, 33). More and more evidence shows that general transcription factors play unique roles in the regulation of tissue-specific gene expression under physiological and pathological conditions. For example, the androgen receptor , via its N-terminal AF1 domain, interacts with basal transcription factors TBP and TFIIF and activates tissue-specific transcription in target tissues and cells (60). Likewise, $TAFII_{17}$ (a component of the TFIID complex), via specific protein-protein interactions with the vitamin D receptor (VDR), increases osteoclast formation from osteoclast precursors in response to 1,25-dihydroxyvitamin D_3 in patients with Paget disease (61). In osteoblasts, bone transcription factors such as Runx2 and ATF4 directly bind to specific DNA sequences in their target gene promoters (*i.e.* OSE2 or NMP2 and OSE1, respectively) and activate osteoblast-specific gene expression, osteoblast differentiation, and bone formation (1, 10–14, 24, 43). Obviously,

Downloaded from www.jbc.org at University of Pittsburgh on July 4, 2008

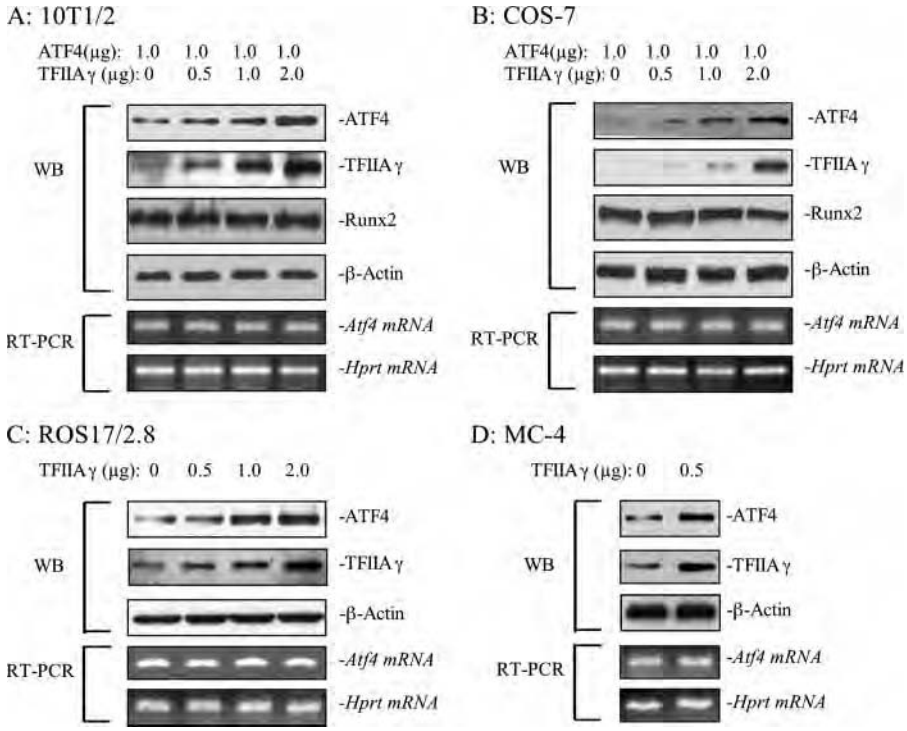

FIGURE 7. **TFIIAγ increases the levels of ATF4 protein.** C3H10T1/2 (*A*) and COS-7 (*B*) cells were transfected with 1 μg of pCMV/ATF4 or pCMV/Runx2 and increasing amounts of FLAG-TFIIAγ expression vector (0, 0.5 1, 2 μg) followed by Western blotting for ATF4, TFIIAγ, Runx2, and β-actin (*top*) or RNA preparation and RT-PCR for *Atf4* and *Hprt* mRNA (*bottom*). ROS17/2.8 (*C*) and MC-4 (*D*) cells were transfected with increasing amounts of FLAG-TFIIAγ expression vector (0, 0.5, 1, and 2 μg). Experiments were repeated three times with similar results.

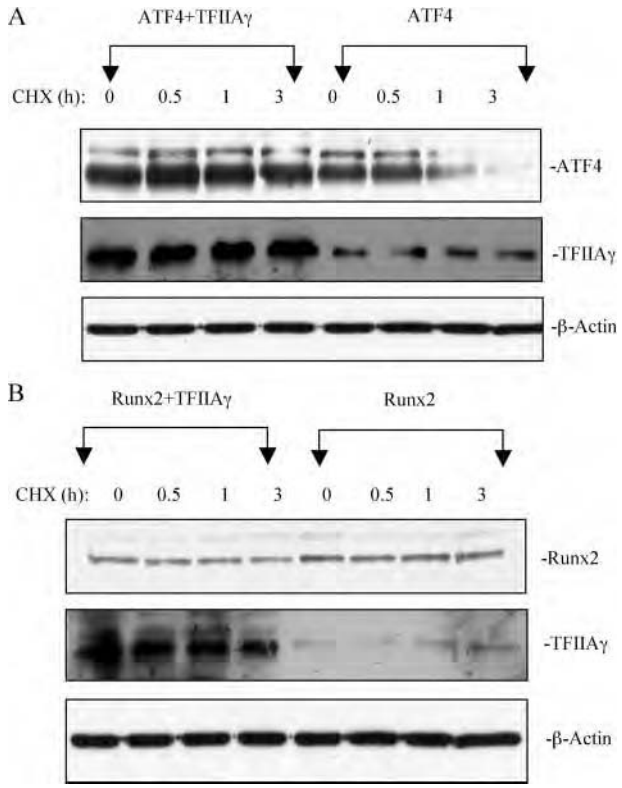

FIGURE 8. **TFIIAγ increases ATF4 protein stability.** C3H10T1/2 cells were transfected with 1.0 μg ATF4 (*A*) or Runx2 (*B*) expression vector with and without 1.0 μg of TFIIA expression vector. After 36 h, cells were treated with 50 μg/ml of protein synthesis inhibitor cycloheximide (*CHX*) and harvested at different time points (0, 1, and 3 h) followed by Western blot analysis for ATF4 and Runx2. Experiments were repeated three times with similar results.

cooperative interactions between osteoblast-specific transcription factors and basal (general) transcriptional machinery are essential for achieving maximal transcription of osteoblast-specific genes. However, little is known about these interactions. Experiments from this study demonstrate that TFIIAγ, which is expressed at high level in osteoblasts, facilitates osteoblast-specific gene expression via two mechanisms. 1) TFIIAγ stabilizes ATF4 and increases the levels of ATF4 proteins. The increased levels of ATF4 further activate Runx2 activity and *Ocn* transcription (25). 2) Through its ability to directly interact with both ATF4 and Runx2, TFIIAγ could recruit these two critical bone transcription factors to the basal transcriptional machinery and greatly enhance osteoblast-specific gene expression. In support of our observation, Guo and Stein (62) showed that Yin Yang-1 (YY1) regulates vitamin D enhancement of *Ocn* gene transcription by interfering with interactions of the VDR with both the VDR element and TFIIB. TFIIB interacts with both VDR and YY1 (63). Likewise, Newberry *et al.* (64) showed that TFIIF (RAP74 and RAP30) mediates Msx2 (a homeobox transcription factor required for craniofacial development) inhibition of *Ocn* promoter activity. Finally, a recent study showed that TFIIB could directly bind to the transactivation domain of Osterix, another important osteoblast transcription factor (65).

TFIIA consists of three subunits designated TFIIAα, TFIIAβ, and TFIIAγ. TFIIAα and TFIIAβ are produced by a specific proteolytic cleavage of the αβ polypeptide that is encoded by *TFIIA-L* (31, 33). TFIIAγ is the smallest subunit with a molecular mass of 12 kDa (42). Although it is encoded by a distinct gene (*TFIIAγ*), TFIIAγ shares a high degree of homology with TFIIAα and TFIIAβ. Interestingly, TFIIAα activates testis-specific gene expression via interactions with a tissue-specific partner, ACT (activator of CREM in testis) and CREM (34). Likewise, TFIIAα enhances human T-cell lymphotropic virus type 1 gene activation through interactions with the Tax protein, a factor associated with adult enhances human T-cell lymphotropic virus type 1 (*HTLV-1*) (35, 66). It remains to be determined whether TFIIAα and TFIIAβ can also interact with ATF4 and Runx2 and similarly activate osteoblast-specific gene expression.

It should be noted that although TFIIAγ belongs to the family of general transcription factors, its expression seems to show some tissue or cell specificity. Osteoblastic cells (MC-4 cells and ROS17/2.8), C3H10T1/2 fibroblasts, and L1 preadipocytes express high levels of TFIIAγ proteins. In contrast, the levels of TFIIAγ protein were undetectable in F9 teratocarcinoma cells

Downloaded from www.jbc.org at University of Pittsburgh on July 4, 2008

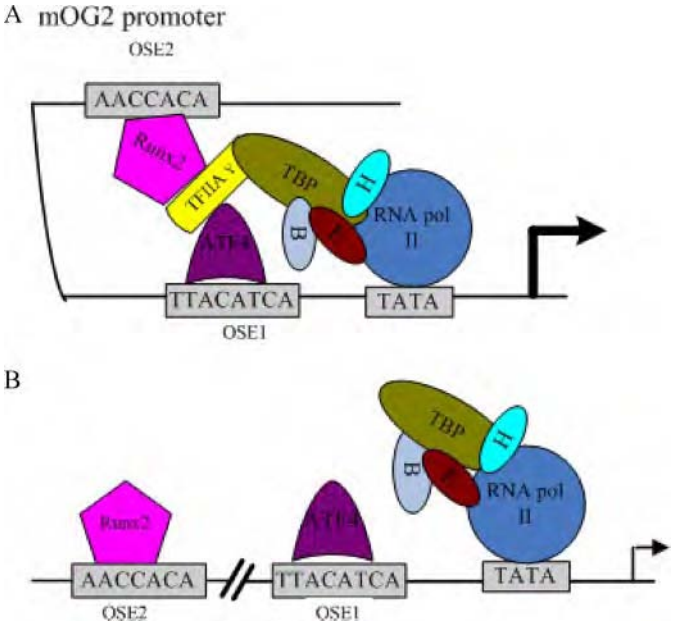

FIGURE 9. **Role of TFIIAγ in osteoblast-specific *Ocn* gene expression.** In osteoblasts, when the level of TFIIAγ is high (*A*), ATF4 and Runx2 are recruited to the transcriptional initiation complex of the *mOG2* promoter through direct binding to TFIIAγ, which in complex with RNA polymerase II and many other basal transcription factors and/or cofactors, including TFIIA, TFIIB, TBP (TFIID), TFIIE, TFIIF, and TFIIH, leads to an increase in transcription. In contrast, when the level of TFIIAγ is low (*B*), ATF4 and Runx2 are not recruited to the basal transcriptional machinery, resulting in a decrease in transcription. Level of TFIIAγ can be regulated by factors to be defined.

and COS-7 on Western blots. The meaning of this observation remains unknown.

These findings suggest that TFIIAγ is a critical factor regulating ATF4 stability and functions as a molecular linker between ATF4 and Runx2 and the basal transcriptional machinery. TFIIAγ may play a unique role in the regulation of osteoblast-specific gene expression and ultimately osteoblast differentiation and bone formation. A working model is proposed in Fig. 9, which summarizes the role of TFIIAγ in osteoblast-specific *mOG2* gene expression. Future study aimed at identifying factors that affect levels and activity of TFIIAγ will allow us to address the functional significance of TFIIAγ in osteoblast function in greater detail.

Acknowledgments—We thank Drs. G. David Roodman (University of Pittsburgh) and Renny T. Franceschi (University of Michigan) for critical reading of the manuscript.

REFERENCES

1. Yang, S., Wei, D., Wang, D., Phimphilai, M., Krebsbach, P. H., and Franceschi, R. T. (2003) *J. Bone Miner. Res.* **18,** 705–715
2. Xiao, G., Jiang, D., Gopalakrishnan, R., and Franceschi, R. T. (2002) *J. Biol. Chem.* **277,** 36181–36187
3. Gilbert, L., He, X., Farmer, P., Rubin, J., Drissi, H., van Wijnen, A. J., Lian, J. B., Stein, G. S., and Nanes, M. S. (2002) *J. Biol. Chem.* **277,** 2695–2701
4. Krishnan, V., Moore, T. L., Ma, Y. L., Helvering, L. M., Frolik, C. A., Valasek, K. M., Ducy, P., and Geiser, A. G. (2003) *Mol. Endocrinol.* **17,** 423–435
5. Xiao, G., Gopalakrishnan, R., Jiang, D., Reith, E., Benson, M. D., and Franceschi, R. T. (2002) *J. Bone Miner. Res.* **17,** 101–110
6. Zhang, X., Sobue, T., and Hurley, M. M. (2002) *Biochem. Biophys. Res. Commun.* **290,** 526–531
7. Hurley, M. M., Tetradis, S., Huang, Y. F., Hock, J., Kream, B. E., Raisz, L. G., and Sabbieti, M. G. (1999) *J. Bone Miner. Res.* **14,** 776–783
8. Montero, A., Okada, Y., Tomita, M., Ito, M., Tsurukami, H., Nakamura, T., Doetschman, T., Coffin, J. D., and Hurley, M. M. (2000) *J. Clin. Investig.* **105,** 1085–1093
9. Yakar, S., Rosen, C. J., Beamer, W. G., Ackert-Bicknell, C. L., Wu, Y., Liu, J. L., Ooi, G. T., Setser, J., Frystyk, J., Boisclair, Y. R., and LeRoith, D. (2002) *J. Clin. Investig.* **110,** 771–781
10. Komori, T., Yagi, H., Nomura, S., Yamaguchi, A., Sasaki, K., Deguchi, K., Shimizu, Y., Bronson, R. T., Gao, Y. H., Inada, M., Sato, M., Okamoto, R., Kitamura, Y., Yoshiki, S., and Kishimoto, T. (1997) *Cell* **89,** 755–764
11. Otto, F., Thornell, A. P., Crompton, T., Denzel, A., Gilmour, K. C., Rosewell, I. R., Stamp, G. W., Beddington, R. S., Mundlos, S., Olsen, B. R., Selby, P. B., and Owen, M. J. (1997) *Cell* **89,** 765–771
12. Mundlos, S., Otto, F., Mundlos, C., Mulliken, J. B., Aylsworth, A. S., Albright, S., Lindhout, D., Cole, W. G., Henn, W., Knoll, J. H., Owen, M. J., Mertelsmann, R., Zabel, B. U., and Olsen, B. R. (1997) *Cell* **89,** 773–779
13. Ducy, P., Zhang, R., Geoffroy, V., Ridall, A. L., and Karsenty, G. (1997) *Cell* **89,** 747–754
14. Banerjee, C., McCabe, L. R., Choi, J. Y., Hiebert, S. W., Stein, J. L., Stein, G. S., and Lian, J. B. (1997) *J. Cell. Biochem.* **66,** 1–8
15. Karpinski, B. A., Morle, G. D., Huggenvik, J., Uhler, M. D., and Leiden, J. M. (1992) *Proc. Natl. Acad. Sci. U. S. A.* **89,** 4820–4824
16. Tsujimoto, A., Nyunoya, H., Morita, T., Sato, T., and Shimotohno, K. (1991) *J. Virol.* **65,** 1420–1426
17. Brindle, P. K., and Montminy, M. R. (1992) *Curr. Opin. Genet. Dev.* **2,** 199–204
18. Hai, T., Wolfgang, C. D., Marsee, D. K., Allen, A. E., and Sivaprasad, U. (1999) *Gene Expr.* **7,** 321–335
19. Meyer, T. E., and Habener, J. F. (1993) *Endocr. Rev.* **14,** 269–290
20. Sassone-Corsi, P. (1994) *EMBO J.* **13,** 4717–4728
21. Ziff, E. B. (1990) *Trends Genet.* **6,** 69–72
22. Yang, X., Matsuda, K., Bialek, P., Jacquot, S., Masuoka, H. C., Schinke, T., Li, L., Brancorsini, S., Sassone-Corsi, P., Townes, T. M., Hanauer, A., and Karsenty, G. (2004) *Cell* **117,** 387–398
23. Ducy, P., and Karsenty, G. (1995) *Mol. Cell. Biol.* **15,** 1858–1869
24. Merriman, H. L., van Wijnen, A. J., Hiebert, S., Bidwell, J. P., Fey, E., Lian, J., Stein, J., and Stein, G. S. (1995) *Biochemistry* **34,** 13125–13132
25. Xiao, G., Jiang, D., Ge, C., Zhao, Z., Lai, Y., Boules, H., Phimphilai, M., Yang, X., Karsenty, G., and Franceschi, R. T. (2005) *J. Biol. Chem.* **280,** 30689–30696
26. Hai, T., and Hartman, M. G. (2001) *Gene* (*Amst.*) **273,** 1–11
27. Lassot, I., Segeral, E., Berlioz-Torrent, C., Durand, H., Groussin, L., Hai, T., Benarous, R., and Margottin-Goguet, F. (2001) *Mol. Cell. Biol.* **21,** 2192–2202
28. Yang, X., and Karsenty, G. (2004) *J. Biol. Chem.* **279,** 47109–47114
29. Lee, D. H., and Goldberg, A. L. (1996) *J. Biol. Chem.* **271,** 27280–27284
30. Rock, K. L., Gramm, C., Rothstein, L., Clark, K., Stein, R., Dick, L., Hwang, D., and Goldberg, A. L. (1994) *Cell* **78,** 761–771
31. Hoiby, T., Zhou, H., Mitsiou, D. J., and Stunnenberg, H. G. (2007) *Biochim. Biophys. Acta* **1769,** 429–436
32. Zhou, H., Spicuglia, S., Hsieh, J. J., Mitsiou, D. J., Hoiby, T., Veenstra, G. J., Korsmeyer, S. J., and Stunnenberg, H. G. (2006) *Mol. Cell. Biol.* **26,** 2728–2735
33. Hoiby, T., Mitsiou, D. J., Zhou, H., Erdjument-Bromage, H., Tempst, P., and Stunnenberg, H. G. (2004) *EMBO J.* **23,** 3083–3091
34. De Cesare, D., Fimia, G. M., Brancorsini, S., Parvinen, M., and Sassone-Corsi, P. (2003) *Mol. Endocrinol.* **17,** 2554–2565
35. Duvall, J. F., Kashanchi, F., Cvekl, A., Radonovich, M. F., Piras, G., and Brady, J. N. (1995) *J. Virol.* **69,** 5077–5086
36. Zhao, C., Irie, N., Takada, Y., Shimoda, K., Miyamoto, T., Nishiwaki, T., Suda, T., and Matsuo, K. (2006) *Cell Metab.* **4,** 111–121
37. Geoffroy, V., Ducy, P., and Karsenty, G. (1995) *J. Biol. Chem.* **270,** 30973–30979
38. Stein, G. S., Lian, J. B., van Wijnen, A. J., and Stein, J. L. (1997) *Mol. Biol. Rep.* **24,** 185–196
39. Banerjee, C., Hiebert, S. W., Stein, J. L., Lian, J. B., and Stein, G. S. (1996)

Downloaded from www.jbc.org at University of Pittsburgh on July 4, 2008

Proc. Natl. Acad. Sci. U. S. A. **93,** 4968–4973
40. Lian, J. B., and Stein, G. S. (2003) *Curr. Pharm. Des.* **9,** 2677–2685
41. Roca, H., Phimphilai, M., Gopalakrishnan, R., Xiao, G., and Franceschi, R. T. (2005) *J. Biol. Chem.* **280,** 30845–30855
42. DeJong, J., Bernstein, R., and Roeder, R. G. (1995) *Proc. Natl. Acad. Sci. U. S. A.* **92,** 3313–3317
43. Xiao, G., Cui, Y., Ducy, P., Karsenty, G., and Franceschi, R. T. (1997) *Mol. Endocrinol.* **11,** 1103–1113
44. Wang, D., Christensen, K., Chawla, K., Xiao, G., Krebsbach, P. H., and Franceschi, R. T. (1999) *J. Bone Miner. Res.* **14,** 893–903
45. Jiang, D., Franceschi, R. T., Boules, H., and Xiao, G. (2004) *J. Biol. Chem.* **279,** 5329–5337
46. Wang, J., Xi, L., Hunt, J. L., Gooding, W., Whiteside, T. L., Chen, Z., Godfrey, T. E., and Ferris, R. L. (2004) *Cancer Res.* **64,** 1861–1866
47. Willis, D. M., Loewy, A. P., Charlton-Kachigian, N., Shao, J. S., Ornitz, D. M., and Towler, D. A. (2002) *J. Biol. Chem.* **277,** 37280–37291
48. Xiao, Z. S., Liu, S. G., Hinson, T. K., and Quarles, L. D. (2001) *J. Cell. Biochem.* **82,** 647–659
49. Xiao, G., Jiang, D., Thomas, P., Benson, M. D., Guan, K., Karsenty, G., and Franceschi, R. T. (2000) *J. Biol. Chem.* **275,** 4453–4459
50. Meyer, T., Carlstedt-Duke, J., and Starr, D. B. (1997) *J. Biol. Chem.* **272,** 30709–30714
51. Lassot, I., Estrabaud, E., Emiliani, S., Benkirane, M., Benarous, R., and Margottin-Goguet, F. (2005) *J. Biol. Chem.* **280,** 41537–41545
52. Garrett, I. R., Chen, D., Gutierrez, G., Zhao, M., Escobedo, A., Rossini, G., Harris, S. E., Gallwitz, W., Kim, K. B., Hu, S., Crews, C. M., and Mundy, G. R. (2003) *J. Clin. Investig.* **111,** 1771–1782
53. Zhao, M., Qiao, M., Harris, S. E., Oyajobi, B. O., Mundy, G. R., and Chen, D. (2004) *J. Biol. Chem.* **279,** 12854–12859
54. Frendo, J. L., Xiao, G., Fuchs, S., Franceschi, R. T., Karsenty, G., and Ducy, P. (1998) *J. Biol. Chem.* **273,** 30509–30516
55. Dobreva, G., Chahrour, M., Dautzenberg, M., Chirivella, L., Kanzler, B., Farinas, I., Karsenty, G., and Grosschedl, R. (2006) *Cell* **125,** 971–986
56. Nakajima, N., Horikoshi, M., and Roeder, R. G. (1988) *Mol. Cell. Biol.* **8,** 4028–4040
57. Buratowski, S., Hahn, S., Guarente, L., and Sharp, P. A. (1989) *Cell* **56,** 549–561
58. Conaway, R. C., and Conaway, J. W. (1989) *Proc. Natl. Acad. Sci. U. S. A.* **86,** 7356–7360
59. Maldonado, E., Ha, I., Cortes, P., Weis, L., and Reinberg, D. (1990) *Mol. Cell. Biol.* **10,** 6335–6347
60. Lavery, D. N., and McEwan, I. J. (2006) *Biochem. Soc. Trans.* **34,** 1054–1057
61. Kurihara, N., Reddy, S. V., Araki, N., Ishizuka, S., Ozono, K., Cornish, J., Cundy, T., Singer, F. R., and Roodman, G. D. (2004) *J. Bone Miner. Res.* **19,** 1154–1164
62. Guo, B., Aslam, F., van Wijnen, A. J., Roberts, S. G., Frenkel, B., Green, M. R., DeLuca, H., Lian, J. B., Stein, G. S., and Stein, J. L. (1997) *Proc. Natl. Acad. Sci. U. S. A.* **94,** 121–126
63. Jurutka, P. W., Hsieh, J. C., Remus, L. S., Whitfield, G. K., Thompson, P. D., Haussler, C. A., Blanco, J. C., Ozato, K., and Haussler, M. R. (1997) *J. Biol. Chem.* **272,** 14592–14599
64. Newberry, E. P., Latifi, T., Battaile, J. T., and Towler, D. A. (1997) *Biochemistry* **36,** 10451–10462
65. Hatta, M., Yoshimura, Y., Deyama, Y., Fukamizu, A., and Suzuki, K. (2006) *Int. J. Mol. Med.* **17,** 425–430
66. Clemens, K. E., Piras, G., Radonovich, M. F., Choi, K. S., Duvall, J. F., DeJong, J., Roeder, R., and Brady, J. N. (1996) *Mol. Cell. Biol.* **16,** 4656–4664

Downloaded from www.jbc.org at University of Pittsburgh on July 4, 2008

A1

AMERICAN SOCIETY FOR BONE AND MINERAL RESEARCH
2025 M Street, NW, Suite 800, Washington, DC 20036-3309, USA
Tel: 202/367-1161, Fax: 202/367-2161, E-mail: ASBMR@asbmr.org

Print this Page for Your Records Close Window

Control/Tracking Number: 07-A-392-ASBMR
Activity: Abstract
Current Date/Time: 4/7/2007 9:40:47 AM

ATF4 Is Required for the Anabolic Actions of PTH on Bone in vivo

Author Block: S. YU[1], M. Luo*[1], R. T. Franceschi[2], D. Jiang*[3], J. Zhang[1], K. Patrene*[1], K. D. Hankenson[4], G. D. Roodman[1], G. Xiao[1]. [1]Medicine, University of Pittsburgh, Pittsburgh, PA, USA, [2]Periodintics and Oral Medicine, University of Michigan, Ann Arbor, MI, USA, [3]Periodontics and Oral Medicine, University of Michigan, Ann Arbor, MI, USA, [4]University of Pennsylvania, Philadelphia, PA, USA.

Abstract: Parathyroid hormone (PTH) is a potent stimulator of bone formation and a proven anabolic agent for the treatment of osteoporosis. However, the mechanism whereby PTH increases bone formation remains poorly understood. Activating transcription factor 4 (ATF4) is a critical factor for bone formation during development and throughout postnatal life. This study examined if ATF4 is required for the anabolic actions of PTH on bone using an Atf4-/- mouse model. Five-day-old wt and Atf4-/- mice were given daily subcutaneous injections of vehicle (saline) or hPTH(1-34) (0.04 Âµg/g body weight) for 28 days. In wt mice, ÂµCT analyses of femurs show that this PTH regimen significantly increased bone volume/tissue volume (BV/TV, 4.3-fold), trabecular thickness (Tb.Th, 50%), trabecualr numbers (Tb.N, 1.5-fold), cortical thickness (Cort.Th, 77%), and cross sectional area (CSA, 24%) and decreased trabecular spacing (Tb.Sp, 1.7-fold). These PTH effects were dramatically reduced or completely abolished in the absence of ATF4. Histological analyses show that PTH displayed potent anabolic effects on tibiae, vertebrae, and calvariae, which were significantly reduced in Atf4-/- mice. At the molecular level, PTH markedly increased levels of osteocalcin (Ocn) and bone sialoprotein (Bsp) mRNA of long bones as measured by quantitative real-time RT/PCR. This increase was completely abolished in the absence of ATF4. This study demonstrates that ATF4 is required for the anabolic actions of PTH on bone in vivo and also suggested that modulation of the levels and activity of ATF4 may have therapeutic significance for the treatment of metabolic bone diseases such as osteoporosis.
:

Author Disclosure Block: **S. Yu**, None.
Payment (Complete): Your credit card order has been processed on Saturday 7 April 2007 at 9:03 AM.
Category (Complete): A - Osteoblasts ; F - Calciotropic and Phosphotropic Hormones and Mineral Metabolism
Preferences (Complete):
***Please select a poster cluster** : 33. F. Calciotropic and Phosphotropic Hormones: Parathyroid and Parathyroid Hormone-Related Peptide

First Name: : Shibing
Last Name: : Yu
E-Mail: : yus@upmc.edu
Phone: : 412-688-6000x814798

Additional Information (Complete):

***First Abstract?** : Yes

***Sponsor First Name** : Guozhi

***Sponsor Last Name** : Xiao

Status: Complete

American Society for Bone and Mineral Research
2025 M Street, NW, Suite 800
Washington, DC 20036-3309 USA

Powered by OASIS, The Online Abstract Submission and Invitation System SM
© 1996 - 2007 Coe-Truman Technologies, Inc. All rights reserved.

A2

Print this Page for Your Records Close Window

Control/Tracking Number: 07-A-389-ASBMR
Activity: Abstract
Current Date/Time: 4/6/2007 11:23:36 PM

TFIIA,ATF4,and Runx2 Synergistically Activate Osteoblast-specific Osteocalcin Gene Expression

Author Block: S. Yu[1], Y. Jiang*[2], M. Luo*[1], Y. Lu[1], J. Zhang[1], G. D. Roodman[1], G. Xiao[1].
[1]Department of Medicine, University of Pittsburgh Medical Center(UPMC), Pittsburgh, PA, USA, [2]Department of Pharmacology, University of Pittsburgh Medical Center(UPMC), Pittsburgh, PA, USA.

Abstract:
Runx2, a member of the runt homology domain family of transcription factors, is a master regulator of osteoblast function and bone formation. Mice lacking Runx2 have no mineralized skeleton due to a complete lack of mature osteoblasts. The expression level of Runx2 protein is regulated by a number of factors including BMPs, FGF-2, IGF-1, TNF-α, TGF-β, and PTH, all of which play important roles in osteoblasts and bone both *in vitro* and *in vivo*. In addition, the activity of Runx2 protein is positively or negatively modulated through protein-protein interactions. Activating transcription factor 4 (ATF4) is an osteoblast-enriched factor which regulates the terminal differentiation and function of osteoblasts. ATF4 knock-out mice have reduced bone mass and bone mineral density (severe osteoporosis) throughout their life. To identify proteins interacting with Runx2, we used a yeast two-hybrid system and identified TFIIA, a general transcriptional factor, as a Runx2-interacting factor. While pull-down assays confirmed that TFIIA physically interacted with Runx2 when both factors were coexpressed in COS-7 cells, surprisingly, it did not activate or inhibit Runx2-dependent transcriptional activity. In contrast, TFIIA unexpectedly activated ATF4, which we recently identified as a Runx2-interacting protein, in a dose-dependent manner. Deletion analysis found that this activation required the presence of the C-terminal 15 amino acid residues of ATF4 molecule. Finally, TFIIA, ATF4, and Runx2 synergistically stimulated the 0.657-kb mOG2 (mouse osteocalcin gene 2) promoter activity and endogenous osteocalcin mRNA expression. In summary, this study demonstrates a novel mechanism through which bone-specific transcription factors and general transcription factors cooperate in regulating osteoblast-specific gene expression.
:

Author Disclosure Block: **S. Yu**, None.

Payment (Complete): Your credit card order has been processed on Friday 6 April 2007 at 10:35 PM.
Category (Complete): A - Osteoblasts ; A - Osteoblasts ; A - Osteoblasts
Preferences (Complete):
***Please select a poster cluster** : 3. A. Osteoblasts: Gene Expression and Transcription Factors
I prefer to give a poster presentation. : True
This abstract is a Cellular Study. : True

Additional Information (Complete):

***First Abstract?** : Yes
***Sponsor First Name** : Shibing
***Sponsor Last Name** : Yu

Status: Complete

American Society for Bone and Mineral Research
2025 M Street, NW, Suite 800
Washington, DC 20036-3309 USA

Powered by OASIS, The Online Abstract Submission and Invitation System SM
© 1996 - 2007 Coe-Truman Technologies, Inc. All rights reserved.